POLITECNICO
DI TORINO

Department of Mechanical and Aerospace Engineering
Master of Science in Automotive Engineering

Master Degree Thesis

Random Fatigue Behavior of Steel by Means of Vibrational Parameters

Supervisors:
Prof. Cristiana **DELPRETE**
Prof. Raffaella **SESANA**

Author:
Mohamad **NASRALLAH**

Torino, March 2018

Acknowledgements

First and foremost, I would like to express my sincere gratitude to God for all the wisdom and perseverance that He has been bestowed upon me during this thesis, and indeed, throughout my life.

I would like to express my deep and respectful gratitude to my thesis advisors, **Prof. Raffaella Sesana** and **Prof. Cristiana Delprete**, for their valuable assistance in pursuing this thesis.

Nevertheless, I am also grateful to Dottore **Francesco Sabatelli**, (mechanical engineering student) for his assistance in doing the experimental tests.

I would like to express my heartfelt gratitude to my friends, **Eng. Ali Hussein**, **Eng. Hassan Darwish,** and **Eng. Seif Salman**, for their great motivation and generous support to me.

Last but not the least, I would like to thank my family for selfless support, encouragement, understanding shown and love given to me during all my life.

Thank you.

Abstract

Estimation of the fatigue life of mechanical components subjected to general load conditions are of great interest in many engineering fields. Fatigue life is estimated by vibration testing. As vibrations may be random in nature in a wide range of applications, random fatigue investigation has the greatest interest. An efficient way of dealing with random vibrations is to use a statistical process to determine the probability of the occurrence of particular amplitudes. In this type of approach, the random vibration can be characterized using a mean, standard deviation and a probability distribution.

The experimental part of this project was consisted in exciting steel alloy specimens with a band-limited ergodic Gaussian white noise using a modal shaker until rupture. Applying some modal analysis techniques, the necessary vibrational parameters were obtained and recorded, thanks to some accelerometers.

The theoretical part was to estimate the fatigue life of the specimen using Miner's rule based on the vibrational parameters collected during the experiments and on statistical representation of the random vibrations applying Steinberg 3-band method. The results were compared to the fatigue life obtained experimentally.

Experiments have shown that the specimen broke in less time than what was predicted theoretically using the same values as in the experiment. The difference might be the result of using a non-precise Wohler's curve.

Table of Contents

Table of Figures

Table of Tables

1 Introduction

Vibration testing is done to introduce a forcing function into a structure, usually with the use of a vibration test shaker or vibration testing machine. These induced vibrations, vibration tests, or shaker tests are used in the laboratory or production floor for a variety of things, including qualifying products during design, meeting standards, regulatory qualifications (e.g. MIL-STD 810, etc.), fatigue testing, screening products, and evaluating performance [1].

The most common types of vibration testing services conducted by vibration test labs are Harmonic and Random. Harmonic (one frequency at a time) tests are performed to survey the structural response of the device under test (DUT). A random (all frequencies at once) test is generally considered to more closely replicate a real-world environment.

Determining the fatigue life of parts under periodic, sinusoidal vibration is a straightforward process in which damage content is calculated by multiplying the stress amplitude of each cycle from harmonic analysis with the number of cycles that the parts experience in the field. The computation is relatively simple because the absolute value of the vibration is highly predictable at any point in time [2].

Vibrations may be random in nature in a wide range of applications, however, such as vehicles traveling on rough roads or industrial equipment operating in the field where arbitrary loads may be encountered. In these cases, instantaneous vibration amplitudes are not highly predictable as the amplitude at any point in time is not related to that at any other point in time. As shown in Figure 1-1, the lack of periodicity is apparent with random vibrations [2].

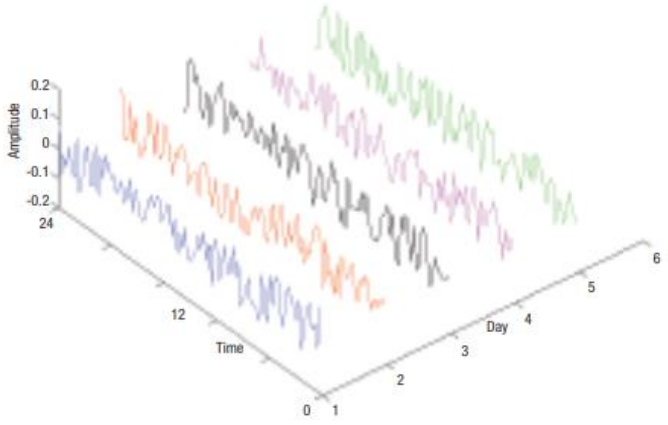

Figure 1-1: Random vibrations measured for vehicle on a rough road

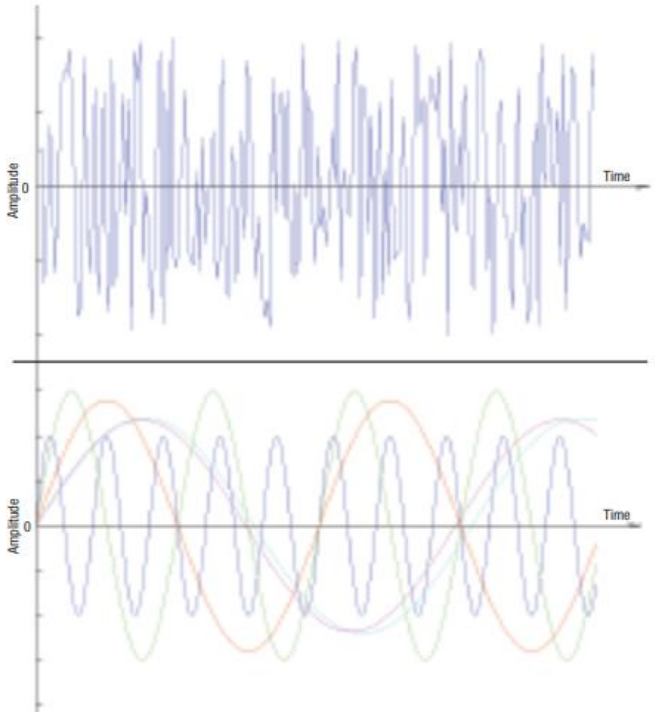

Figure 1-2: Random time–history can be represented as a series of overlapping sinusoidal curves

The complex nature of random vibrations is demonstrated with a Fourier analysis of the random time–history shown in Figure 1-2, revealing that the random motion can be represented as a series of many overlapping sine waves, with each curve cycling at its own frequency and amplitude. With these multiple frequencies occurring at the same time, the structural resonances of different components can be excited simultaneously, thus increasing the potential damage of random vibrations.

Because of the mathematical complexity of working with these overlapping sine curves to find instantaneous amplitude as an exact function of time, a more efficient way of dealing with random vibrations is to use a statistical process to determine the probability of the occurrence of particular amplitudes. In this type of approach, the random vibration can be characterized using a mean, the standard deviation and a probability distribution. Individual vibration amplitudes are not determined. Rather, the amplitudes are averaged over a large number of cycles and the cumulative effect determined for this time period. This provides a more practical process for characterizing random vibrations than analyzing an unimaginably large set of time–history data for many different vibration profiles.

An important aspect of such a statistical representation is that most random processes follow a Gaussian probability distribution. This aspect has a great rule in this work since the excitation random signal, in the fatigue tests done, was the Gaussian White Noise.

Representing the random signals in this manner is sometimes called a zero-mean Gaussian process, since the mean value of the signals centers at zero of the histogram, as do the random signal responses, which are usually described in terms of standard deviation (or sigma value) of the distribution. Figure 1-3 shows how the Gaussian distribution relates to the magnitude of the acceleration levels expected for random vibration. It is important to note that the Gaussian probability distribution does not indicate the random signal's frequency content. That is the function of the power spectral density analysis.

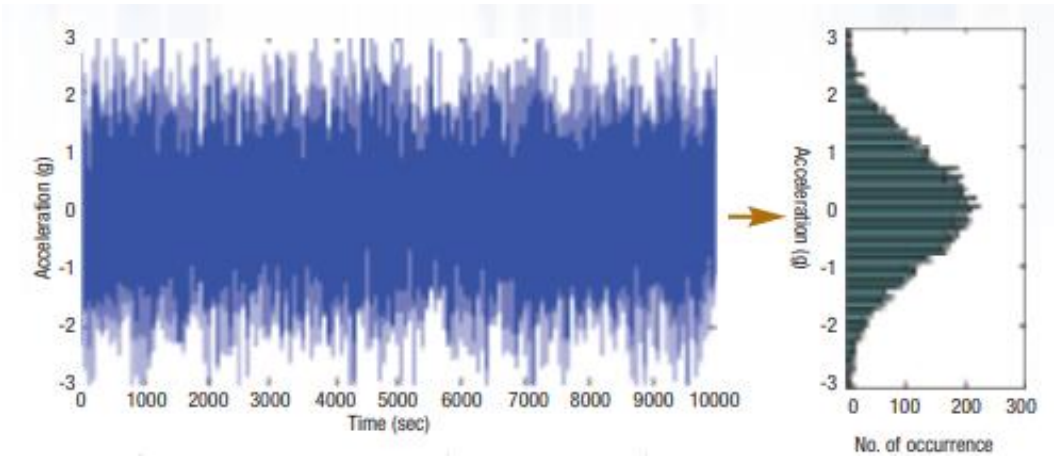

Figure 1-3: Gaussian distribution (right) of random signal (left):

The usual way to describe the severity of damage for random vibration is in terms of its power spectral density (PSD), a measure of a vibration signal's power intensity in the frequency domain.

Random vibration analysis is usually performed over a large range of frequencies — from 20 to 2,000 Hz, for example. Such a study does not look at a specific frequency or amplitude at a specific moment in time but rather statistically looks at a structure's response to a given random vibration environment. Certainly, we want to know if there are any frequencies that cause a large random response at any natural frequencies, but mostly we want to know the overall response of the structure. The square root of the area under the PSD curve (grey area) in Figure 1-4 gives the root mean square (RMS) value of the acceleration, or Grms, which is a qualitative measure of intensity of vibration.

In vibration theory, the modal analysis method allows huge simplifications in studying the vibratory response of systems from both deterministic and random excitations. Since the end of the last century, experimental modal analysis techniques received a special attention and started to be used in many practical applications, with satisfactory results.

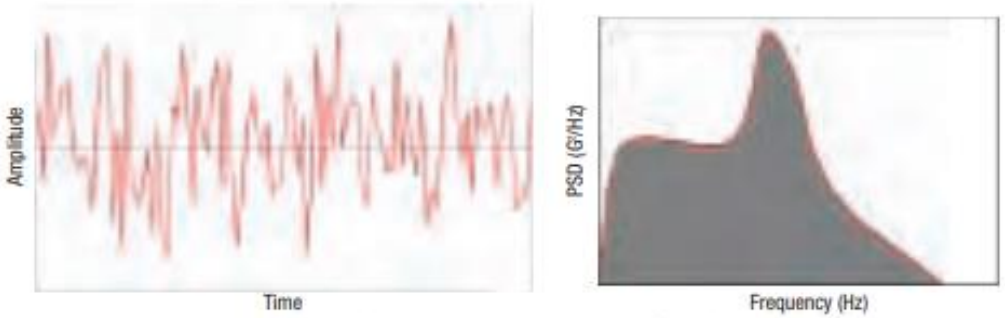

Figure 1-4: Random time–history (left), power special density (PSD) of a random time-history (right)

The objective of this thesis is to develop a new constitutive model and a new damage model for high cycle fatigue behavior of steel alloy starting from random fatigue tests.

In brief, the purpose of this work is to start a bibliographic research in the field of vibration, modal analysis and fatigue, to discover and get familiar with these areas (chapter 2). Then, to do the predefined experimental tests and simulations on steel specimens; first to find the modal parameters, then to perform the random fatigue tests (chapter 3). Finally, to process the results by the chosen fatigue model and to correlate the results obtained theoretically with those obtained experimentally (chapter 4).

This work which last six months was to set the foundations for future studies by moving further from the first steps already taken by previous students in the DIMEAS Laboratory with the same equipment set.

2 Literature Review

2.1 Introductory Concepts on Vibrations

The vibrations of linear systems fall into two categories – free and forced. Free vibrations occur when a system vibrates in the absence of any externally applied forces (i.e. the externally applied force is removed and the system vibrates under the action of internal forces). A finite system undergoing free vibrations will vibrate in one or more of a series of specific patterns. Each of these specific vibration patterns is called a mode shape and it vibrates at a constant frequency, which is called a natural frequency [3]. These natural frequencies are properties of the finite system itself and are related to its mass and stiffness (inertia and elasticity). It is interesting to note that if a system were infinite it would be able to vibrate freely at any frequency (this point is relevant to the propagation of sound waves) [3]. Forced vibrations, on the other hand, take place under the excitation of external forces. These excitation forces may be classified as being (i) harmonic, (ii) periodic, (iii) non-periodic (pulse or transient), or (iv) stochastic (random). Forced vibrations occur at the excitation frequencies, and it is important to note that these frequencies are arbitrary and therefore independent of the natural frequencies of the system [3]. The phenomenon of resonance is encountered when a natural frequency of the system coincides with one of the exciting frequencies.

When the energy of a vibrating system is gradually dissipated by friction and other resistances, the vibrations are said to be damped. The vibrations gradually reduce or change in frequency or intensity or cease and the system rests in its equilibrium position. An example of this type of vibration is the vehicular suspension dampened by the shock absorber.

2.2 Single Degree-of-Freedom (SDOF) System

The fundamentals of vibration analysis can be understood by studying the simple mass-spring-damper model, Figure 2-1 [4]. Indeed, even a complex structure such as an automobile body can be modelled as a "summation" of simple mass-spring-damper models. The mass-spring-damper model is an example of a simple harmonic oscillator. The mathematics used to describe its behavior is identical to other simple harmonic oscillators such as the RLC circuit.

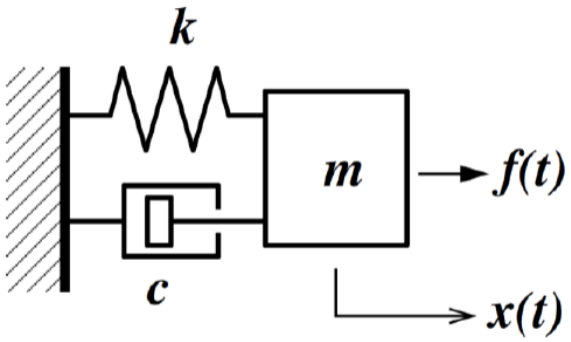

Figure 2-1: Mass–spring–damper model; **k** is the linear elastic stiffness coefficient, **m** is the object's mass, **c** is the linear viscous damping coefficient, and **f(t)** is the external excitation force (in case of free vibration, $\mathbf{f(t) = 0}$)

The mass–spring–damper model, shown in Figure 1.1, is called a single degree of freedom (SDOF) model since the mass is assumed to only move up and down. In more complex systems, the system must be discretized into more masses that move in more than one direction, adding degrees of freedom. This latter system is called a multiple degree of freedom system and will be discussed in section 2.4.

The step-by-step mathematical derivations are not included in this thesis, as they are not the point of interest. A detailed description can be found in numerous text books and articles. Some of these references are included in the bibliography [3] [5] [4] [6] [7] [8].

The equation of motion for translation oscillations of the single degree-of-freedom system in Figure 2-1 is:

$$\boldsymbol{m\ddot{x}(t) + c\dot{x}(t) + kx(t) = f(t)} \tag{1}$$

The natural frequency $\boldsymbol{f_n}$ of the system is defined as:

$$\boldsymbol{\omega_0 = 2\pi f_n = \sqrt{k/m}} \tag{2}$$

The damping ratio $\boldsymbol{\zeta}$, defined as the ratio of the actual damping $\boldsymbol{c}$ to the critical damping $\boldsymbol{c_c = 2\sqrt{mk}}$:

$$\boldsymbol{\zeta = c/c_c} \tag{3}$$

2.2.1 Free Vibration [4]

Considering the case of free vibration, i.e. $\boldsymbol{f(t) = 0}$, eq. (1) can be written as:

$$\boldsymbol{m\ddot{x}(t) + c\dot{x}(t) + kx(t) = 0} \tag{4}$$

Based on equation (4) the SDOF system can be classified as:

- Undamped ($\boldsymbol{\zeta \to 0}$): system with constant amplitude oscillations;
- Underdamped ($\boldsymbol{\zeta < 1}$ & $\boldsymbol{c < c_c}$): characterized by a cosinusoidal decay oscillation;

- Overdamped ($\zeta > 1$ & $c > c_c$): exponential decay with no oscillation but which takes more time to reach the equilibrium position when compared to the critically damped system;
- Critically damped ($\zeta = 1$ & $c = c_c$): system returns to the equilibrium position quick with no overshoot or oscillation.

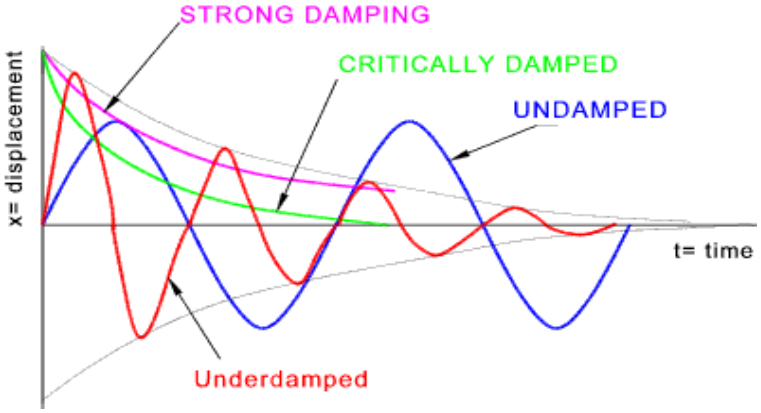

Figure 2-2: Free response of single degree-of-freedom system.

Figure 2-2 shows a graphical representation of the free response of SDOF system with different damping ratios. For the purposes of the present thesis, only under-damped systems will be considered, since all the studied phenomena on the experimental tests have small damping ratio values.

2.2.2 Forced Vibration with Harmonic Excitation [4]

We consider the periodic forcing function:

$$f(t) = F \sin(2\pi f t) \tag{5}$$

Substituting equation (5) in equation (1), the steady state solution of this problem can be written as:

$$x(t) = X \sin(2\pi f t + \phi) \tag{6}$$

The result states that the mass will oscillate at the same frequency, f, of the applied force, but with a phase shift $\emptyset$. X is the vibration amplitude. X and ϕ can be expressed as:

Amplitude:
$$X = \frac{F}{k} \frac{1}{\sqrt{(1 - r^2)^2 + (2\zeta r)^2}} \tag{7}$$

Phase:
$$\phi = \tan^{-1}\left(\frac{2\zeta r}{1 - r^2}\right) \tag{8}$$

where "r" is defined as the ratio of the harmonic force frequency over the undamped natural frequency of the mass–spring–damper model:

$$r = f / f_n \tag{9}$$

2.2.3 Frequency Response Function

The plot of these functions (7) and (8), Figure 2-3, called "the Frequency Response of the system (FRF)", presents one of the most important features in forced vibration. In a lightly damped system when the forcing frequency nears the natural frequency ($\boldsymbol{r \approx 1}$), the amplitude of the vibration can get extremely high. This phenomenon is called resonance (subsequently the natural frequency of a system is often referred to as the resonant frequency).

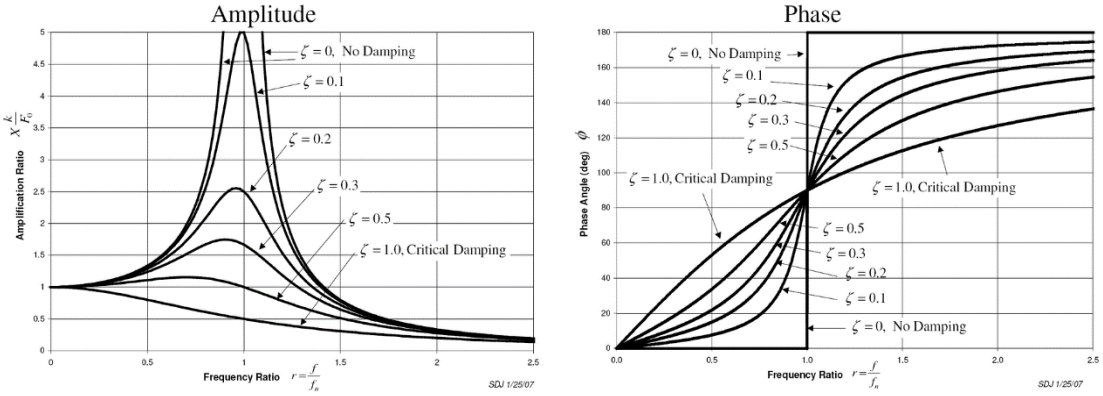

Figure 2-3: Forced Vibration Response

So far in this sub-section, solutions have been sought for the output steady-state displacement, $\boldsymbol{X}$. The complex ratio of the output displacement to the input force, $\boldsymbol{X/F}$, i.e. equation (7), is commonly referred to as a receptance. There are a range of different force–response relationships that are of general engineering interest. In many applications in noise and vibration, in addition to the receptance, the mobility (velocity/force; $\boldsymbol{V/F}$) and the inertance (acceleration/force; $\boldsymbol{A/F}$) are often of interest.

2.2.4 Quality factor

It can be shown that the steady-state amplitude, X, is a maximum when

$$\boldsymbol{r = \sqrt{1 - 2\zeta^2}} \tag{10}$$

The maximum value of $\boldsymbol{X}$ is:

$$\boldsymbol{X_r = \frac{X_0}{2\zeta\left(\sqrt{1-\zeta^2}\right)}} \tag{11}$$

and the corresponding phase angle at $\boldsymbol{X = X_r}$ is:

$$\boldsymbol{\varphi = \tan^{-1}\left(\frac{\sqrt{1-2\zeta^2}}{\zeta}\right)} \tag{12}$$

where $\boldsymbol{X_0 = F/k}$. For most practical situations, however, $\boldsymbol{\zeta}$ is small (<0.05):

$$\boldsymbol{X_r \approx \frac{X_0}{2\zeta} \quad \& \quad \varphi \approx \tan^{-1}\left(\frac{1}{\zeta}\right)} \tag{13}$$

For these cases of small damping, amplitude resonance and phase resonance are assumed to be equal, i.e. $\boldsymbol{\varphi \approx 90°}$, and therefore $\boldsymbol{\omega \approx \omega_n}$. The magnification factor at resonance is thus $\sim \boldsymbol{1/2\zeta}$ and it is called the $\boldsymbol{Q}$ factor or the quality factor, i.e.:

$$\frac{\boldsymbol{X_r}}{\boldsymbol{X_0}} = \frac{\boldsymbol{1}}{\boldsymbol{2\zeta}} = \boldsymbol{Q} \tag{14}$$

The quality factor is described physically as a measure of the sharpness of the response at resonance and is a measure of the system's damping. The points where the magnification factor is reduced to $\boldsymbol{1/\sqrt{2}}$ of its peak value (or the −3 dB points) are defined as the half-power points. The damping in a system can thus be obtained from the **half-power bandwidth**. This is illustrated in Figure 2-4. By solving equation (7) for $\boldsymbol{Xmax/\sqrt{2}}$, where $\boldsymbol{X_{max} = X_r/X_0}$, the half-power frequencies ($\boldsymbol{\omega_1}$ and $\boldsymbol{\omega_2}$) can be obtained. They are

$$\boldsymbol{\omega_{1,2} = (1 \pm \zeta)\omega_n}, \tag{15}$$

therefore,

$$\boldsymbol{Q = \frac{1}{2\zeta} = \frac{\omega_n}{\omega_2 - \omega_1}} \tag{16}$$

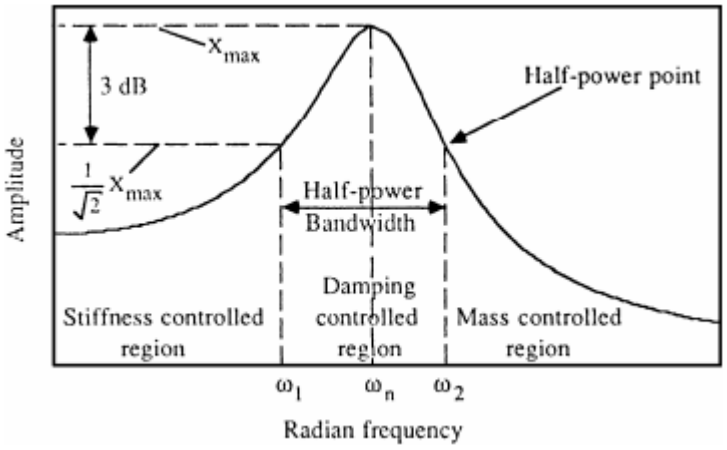

Figure 2-4: Half-power bandwidth and half-power points for a linear oscillator

2.3 Forced Vibration with Random Excitation [3]

As already mentioned before, excitation forces may be classified as being harmonic, periodic, non-periodic (pulse or transient), or stochastic (random).

The response of a one-degree-of-freedom system harmonic signals has been summarized in section 2.2.2. The cases of periodic and non-periodic signals are beyond the scope of this thesis, as random excitations are the point of interest. However, these signals are still deterministic and can therefore be expressed by an explicit mathematical relationship.

Quite often, in noise and vibration analysis, the input signal to some system cannot be described by an explicit mathematical relationship. It is random in nature (i.e. the time history of the signal is neither periodic nor transient but is continuous and does not repeat itself) and should be described in terms of probability statements and statistical averages – this class of vibrations is

termed random vibrations. Also, if the input to a system is random, its output vibrations will also be random. Some typical examples of random vibrations are the turbulent flow over an aircraft body; the response of ships to ocean waves…etc. A time history of a typical random signal containing numerous frequency components is illustrated in Figure 2-5.

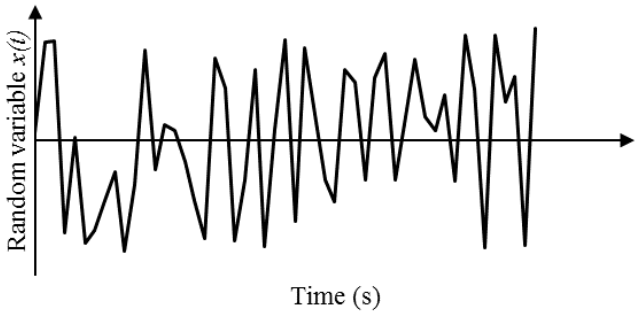

Figure 2-5: A time history of a typical random signal.

An individual time history of a random signal is called a sample record, and a collection of several such records constitutes an ensemble average of a random, or a stochastic, process. A random process can be:

i. ergodic (or strictly stationary) if all the probability distributions associated with it are time-invariant;
ii. weakly stationary if only its first and second order probability distributions are invariant with time;
iii. non-stationary when its probability distributions are not stationary with respect to a change of the time scale, i.e. they vary with time.

Most random physical phenomena that are of interest to engineers can be approximated as being stationary – if a signal is very long compared with the period of the lowest frequency component of interest, it is approximately stationary. Therefore, only the random vibrations of stationary signals (ergodic) will be presented in this thesis. A Flowchart illustrating the different types of input and output signals can be found in Appendix A

Four types of statistical functions are used to describe random signals:

i. mean-square values and the variance – they provide information about the amplitude of the signal;
ii. probability distributions – they provide information about the statistical properties of the signal in the amplitude domain;
iii. correlation functions – they provide information about the statistical properties of the signal in the time domain;
iv. spectral density functions – they provide information about the statistical properties of the signal in the frequency domain.

Throughout this section a linear system with a single input and a single output will be considered. The input will be assumed to be a random signal, $\boldsymbol{x}(\boldsymbol{t})$, and the output will be defined as $\boldsymbol{y}(\boldsymbol{t})$. The system will be modelled as a SDOF mass–spring–damper.

2.3.1 Probability Density Function (PDF)

The expected or mean value of a function $x(t)$ is given by:

$$E[x(t)] = \frac{1}{T}\int_0^T x(t)dt = \int_{-\infty}^{\infty} xp(x)\,dx \tag{17}$$

where $p(x)$ is the probability density function. It specifies the probability, $p(x)\,dx$, that a random variable lies in the range x to $x + dx$.

For a stationary random process, $E[x(t)] = E[x]$. This is because a stationary random process is time-invariant. It is sometimes referred to as the first statistical moment.

The second statistical moment, or the mean-square value, $E[x^2]$, is the average value of x^2 and is given by:

$$E[x^2(t)] = \frac{1}{T}\int_0^T x^2dt = \int_{-\infty}^{\infty} x^2p(x)\,dx \tag{18}$$

The positive square root of $E[x^2]$ is the **Root-Mean-Square (RMS)** value of the signal. The standard deviation σ of $x(t)$, and the variance, σ^2, are defined by:

$$\sigma^2 = E[x^2] - \{E[x]\}^2 \tag{19}$$

2.3.2 Auto-Correlation Function

The auto-correlation function for a random signal, $x(t)$, provides information about the degree of dependence of the value of x at some time t on its value at some other time $+\tau$. For a stationary random signal, the auto-correlation depends upon the time separation, and is independent of absolute time. It is defined as:

$$R_{xx}(\tau) = E\big(x(t)\,x(t+\tau)\big) = \lim_{T\to\infty}\frac{1}{T}\int_0^T x(t)\,x(t+\tau)dt \tag{20}$$

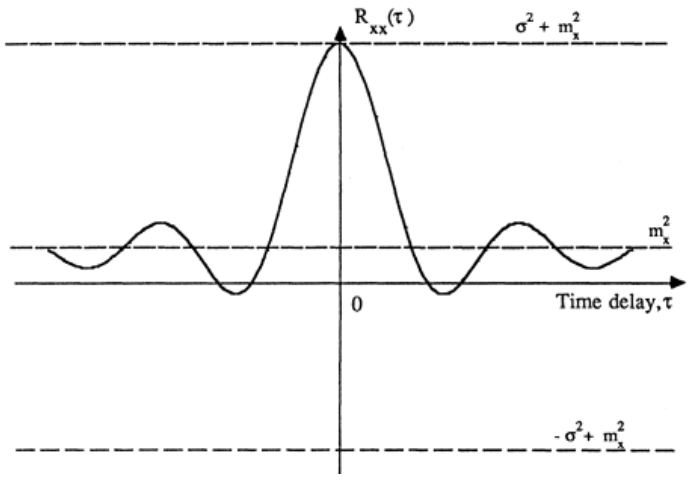

Figure 2-6: A typical auto-correlation function for a stationary random signal.

The auto-correlation function is an even function, it does not contain any phase information, and its maximum value always occurs at $\boldsymbol{\tau} = \mathbf{0}$. For periodic signals, $\boldsymbol{R_{xx}(\tau)}$ is always periodic, and for random signals it always decays to zero for large values of $\boldsymbol{\tau}$. It is therefore a useful tool for identifying deterministic signals which would otherwise be masked in a random background. A typical auto-correlation signal is illustrated in Figure 2-6.

2.3.3 Power Spectral Density Function (PSD)

The spectral density function is the Fourier transform of the correlation coefficient. A general Fourier transform pair, $\boldsymbol{X(\omega)}$ and $x(t)$ is defined as:

$$\boldsymbol{X(\omega)} = \frac{1}{2\pi}\int_{-\infty}^{+\infty} x(t)\, e^{-i\omega t} dt \tag{21}$$

and

$$x(t) = \int_{-\infty}^{+\infty} \boldsymbol{X(\omega)} e^{i\omega t} dt \tag{22}$$

$\boldsymbol{X(\omega)}$ is the Fourier transform of $x(t)$ and it is a complex quantity. Classical Fourier analysis also introduces the condition that:

$$\int_{-\infty}^{+\infty} |x(t)|\, d\tau < \infty \tag{23}$$

i.e. classical theory is valid for functions which are absolutely integrable and decay to zero when $|t| \to \infty$. Stationary random signals do not decay to zero with time. This problem is overcome by Fourier analysing the correlation function instead (the correlation function of a random signal decays to zero with increasing τ). It is important to note that the frequency content of the stationary random signal is not lost in the process.

The Fourier transform of $R_{xx}(\tau)$ and its inverse are thus given by:

$$\boldsymbol{S_{xx}(\omega)} = F\big(R_{xx}(\tau)\big) = \frac{1}{2\pi}\int_{-\infty}^{+\infty} R_{xx}(\tau) \cdot e^{-i\omega t} d\tau \tag{24}$$

$\boldsymbol{S_{xx}(\omega)}$ is the auto-spectral density of the $x(t)$ random signal and it is a function of frequency. The auto-spectral density is widely used in noise and vibration analysis. The area under an auto-spectrum is the mean-square value of a signal.

It should be pointed out at this stage that the experimental estimation of spectra from measured data does not follow the above mentioned formal mathematical route of obtaining the spectra from the correlation function. With the development of the fast Fourier transform (FFT) technique, digital estimates of spectra can be directly obtained from the time histories with suitable computer algorithms.

2.3.4 Frequency Response Function (FRF)

Consider an arbitrary input signal, $x(t)$, to a linear system such that the condition in eq. (23). Its Fourier transform, $\boldsymbol{X(\omega)}$, is given by eq. (21).

For a linear system, there is a relationship between the Fourier transforms of the input signal, $\boldsymbol{X(\omega)}$, and the output signal, $\boldsymbol{Y(\omega)}$. This relationship is:

$$\boldsymbol{Y(\omega)} = \boldsymbol{H(\omega)X(\omega)} \tag{25}$$

where $\boldsymbol{H(\omega)}$ is the Frequency Response Function (FRF) of the linear system. $\boldsymbol{H(\omega)}$ can be receptance, mobility, inertance etc... as described in section 2.2.3. The output signal, $\boldsymbol{y(t)}$, from the linear system can subsequently be obtained by inverse Fourier transforming equation.

From the receptance FRF, it is possible to calculate the other quantities using derivatives, and the following expressions are obtained:

Receptance: $$\boldsymbol{R(\omega)} = \frac{\boldsymbol{X(\omega)}}{\boldsymbol{F(\omega)}} \tag{26}$$

Mobility: $$\boldsymbol{V(\omega)} = \frac{\boldsymbol{\dot{X}(\omega)}}{\boldsymbol{F(\omega)}} = \boldsymbol{i\omega}\frac{\boldsymbol{X(\omega)}}{\boldsymbol{F(\omega)}} \tag{27}$$

Inertance: $$\boldsymbol{A(\omega)} = \frac{\boldsymbol{\ddot{X}(\omega)}}{\boldsymbol{F(\omega)}} = -\boldsymbol{\omega^2}\frac{\boldsymbol{X(\omega)}}{\boldsymbol{F(\omega)}} \tag{28}$$

2.3.5 Ergodic White Gaussian Noise

In probability theory, the normal (or Gaussian) distribution is a very common continuous probability distribution function. A typical Gaussian distribution curve is illustrated in Figure 2-7. Gaussian random process is a random process in which, for any time instant on an ensemble, the random variables follow a Gaussian distribution. It can be proved that if the excitation of a linear system is a Gaussian random process, the response is Gaussian [7].

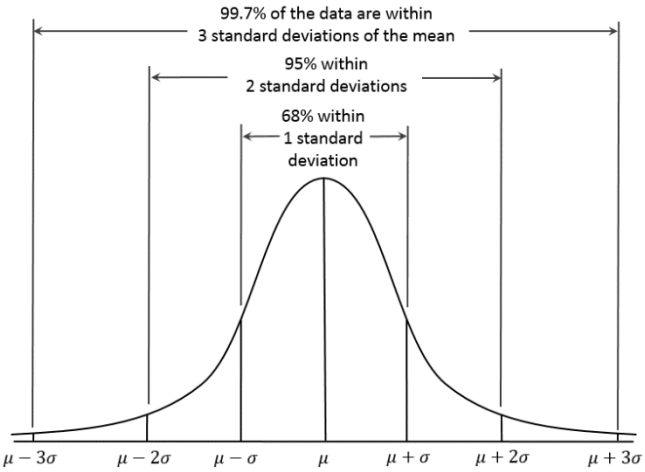

Figure 2-7: Gaussian Probability Density Function

White Noise is a random signal having equal intensity at different frequencies, giving it a constant power spectral density [9]. White noise refers to a statistical model for signals and signal sources, rather than to any specific signal. White noise draws its name from white light [10].

In discrete time, white noise is a discrete signal whose samples are regarded as a sequence of serially uncorrelated random variables with zero mean and finite variance. If each of these samples has a normal distribution with zero mean, the signal is said to be Gaussian white noise [11].

Typically, the PSD of a white Gaussian noise is wide and flat, Figure 2-8a. A PSD that extends from $-\infty$ to $+\infty$ is not realistic. Therefore, noise is considered only in the interested bandwidth. An example of passband white Gaussian noise PSD is illustrated in Figure 2-8b.

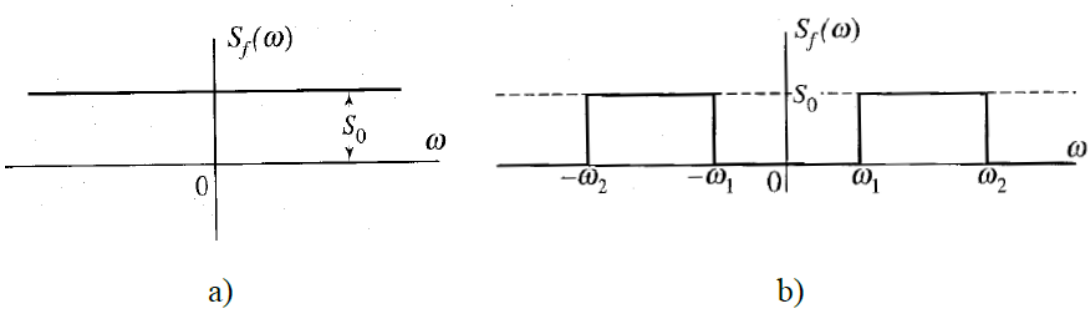

Figure 2-8: PSD of (a) an ideal white noise, and (b) a passband white noise

In the experimental tests, which will be described later, random excitations were done by applying ergodic white Gaussian noise to the testing specimens.

2.4 Multiple Degree of Freedom (MDOF) System

Differently from the SDOF systems, multi degrees of freedom systems, as the one in Figure 2-9, require more than one independent coordinate to describe its parts position. Systems with a finite number of degrees of freedom are called discrete.

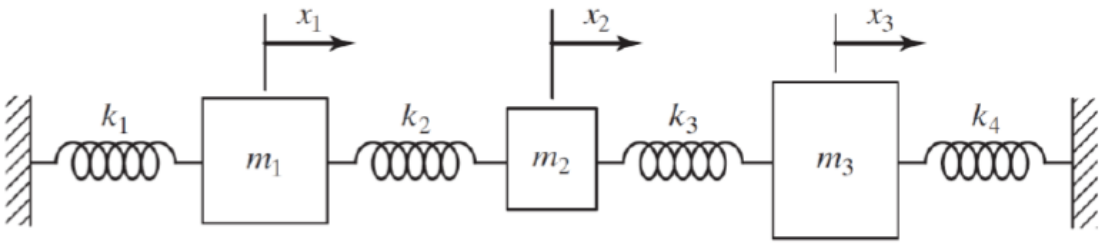

Figure 2-9: Multiple degree of freedom system

Many real systems, especially those involving continuous elastic members, have an infinite number of degrees of freedom, and are called continuous or distributed systems. Most of the time, these continuous systems are

approximated by discrete systems with multiple degrees of freedom instead of dealing with a continuous problem, and the solutions are obtained in a simpler manner, although not exact. However, the advent of computers made possible the development of numerical methods for solving in some reasonable time systems with a great number of degrees of freedom, improving the result's accuracy.

Different methods exist to approximate a continuous system to a MDOF system, such as the lumped-parameter method of the finite element method. In this thesis, the latter was used, and it consists on "replacing the geometry of the system by large number of small elements. By assuming a simple solution within each element, the principles of compatibility and equilibrium are used to find an approximate solution to the original system" [6].

In any case, it's possible to derive a set of n equations of motion, where n is the number of degrees of freedom of the system. These equations can be expressed is matrix form as:

$$[\boldsymbol{M}]\{\ddot{\boldsymbol{x}}(\boldsymbol{t})\} + [\boldsymbol{C}]\{\dot{\boldsymbol{x}}(\boldsymbol{t})\} + [\boldsymbol{K}]\{\boldsymbol{x}(\boldsymbol{t})\} = \{\boldsymbol{F}(\boldsymbol{t})\} \tag{29}$$

where $[\boldsymbol{M}], [\boldsymbol{C}]$ and $[\boldsymbol{K}]$ are the called mass, damping and stiffness matrices, respectively, and $\{\ddot{\boldsymbol{x}}(\boldsymbol{t})\}, \{\dot{\boldsymbol{x}}(\boldsymbol{t})\}, \{\boldsymbol{x}(\boldsymbol{t})\}$ and $\{\boldsymbol{F}(\boldsymbol{t})\}$ are the acceleration, the velocity, the displacement and the force vectors respectively.

In the general case, the matrices $[\boldsymbol{M}], [\boldsymbol{C}]$ and $[\boldsymbol{K}]$ are fully populated and equation (29) denotes a system of n coupled second-order ordinary differential equations. These equations can be decoupled using a procedure called modal analysis, which requires the natural frequencies and normal modes or natural modes of the system [8].

2.5 Modal Analysis

Modal analysis is the study of a structure in terms of its natural characteristics which are the frequency, damping and mode shapes i.e. its dynamic properties [12].

Modal analysis is the field of measuring or calculating and analyzing the dynamic response of structures during excitation. Examples would include measuring the vibration of a car's body when it is attached to an electromagnetic shaker, analysis of unforced vibration response of vehicle suspension [13]. Modern day experimental modal analysis systems are composed:

- sensors such as transducers (typically accelerometers, load cells), or non-contact via a laser vibrometer, or stereo photogrammetric cameras
- data acquisition system and an analogue-to-digital converter front end (to digitize analogue instrumentation signals) and
- host PC (personal computer) to view the data and analyses it.

Typical excitation signals can be classed as impulse, broadband, swept sine, chirp, and possibly others. Each has its own advantages and disadvantages.

Where structural resonances occur, there will be an amplification of the response, clearly seen in the response spectra. Figure 2-10 illustrates an example of a frequency response function, where the peaks represents the resonances or the natural frequencies of the tested structure. Using the response spectra and force spectra, a transfer function can be obtained. The transfer function (or frequency response function (FRF)) is often curve fitted to estimate the modal parameters i.e. the modal frequency (resonance), the modal damping (damping at resonance), and the mode shape [14]; however, there are many methods of modal parameter estimation and it is the topic of much research.

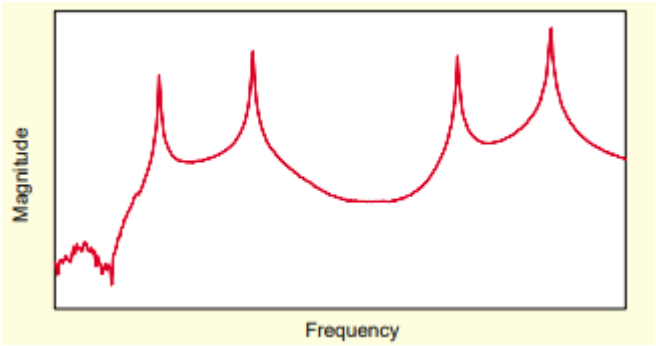

Figure 2-10: A typical example of frequency response spectrum

2.5.1 Modal Parameters Estimation Methods

Modal parameter estimation is the process of determining the modal parameters from experimentally measured data. These techniques, also called curve fitting, have developed greatly during the past 30 years.

The most widespread classification of modal parameter identification methods is between frequency domain methods and time domain methods. The technique used in this work is a frequency domain method so-called Peak-Picking technique. It was used for its simplicity and compatibility to the available equipment [15].

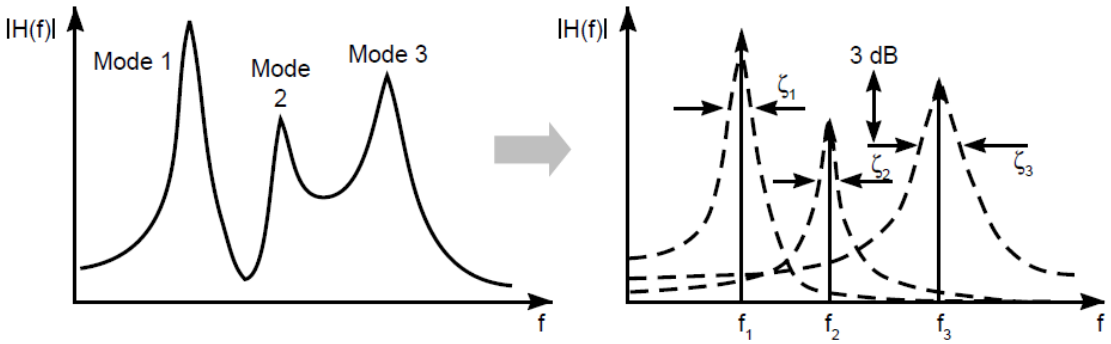

Figure 2-11: The frequency response of simple structures can be split up into individual modes, each mode behaving as a SDOF system

For lightly damped systems without closely spaced modes it can be assumed that near a natural frequency, the overall vibration tends to be dominated by the mode of resonance, whereas the other modes' influence is negligible. So, this mode can be idealized as an independent SDOF system, as shown in Figure 2-11, and the overall response of the structure at any frequency is the sum of the contributions of each mode. This is called the superposition principle [14].

The modal frequencies can be estimated from the frequency response data by observing the frequency at which any of the following trends occur [16]:

- The magnitude of the frequency response is a maximum;
- The imaginary part of the frequency response is a maximum or minimum;
- The real part of the frequency response is zero;
- The phase of the frequency response is 90°.

A graphical representation of these trends is shown in Figure 2-12.

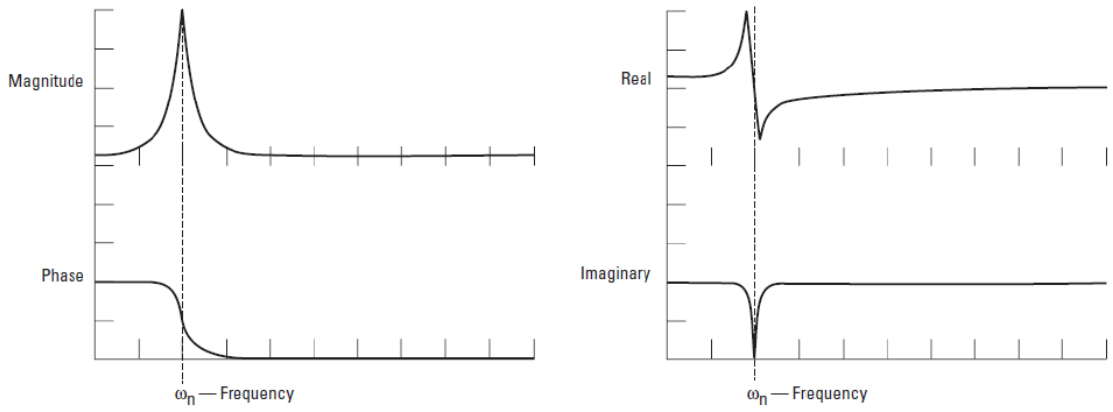

Figure 2-12: Modal frequency identification on an idealized SDOF system

A commonly used technique to extract the modal damping from the FRF is the half-power bandwidth or 3dB method, in which each of the idealized SDOF systems that compose the measured FRF is analyzed separately. This method is described in section 2.2.4.

From the measured modal damping, it is possible to calculate the equivalent loss factor $\boldsymbol{\eta}$ from the following equation, as pointed out by [17]:

$$\boldsymbol{\eta = 2\zeta \cdot \sqrt{1 - \zeta^2}} \tag{30}$$

To estimate the modal shape, one of the simplest method is called Quadrature Picking and it's based on the fact that the FRF of a SDOF system at resonance is purely imaginary, and as a result, this value is proportional to the modal displacement. Consequently, by examining the magnitude of the imaginary part of the FRF in the resonant frequencies at several points on the structure, the relative modal displacement at each point can be found. From these displacements, the mode shapes can be established. The procedure can then be repeated to determine all the required mode shapes [14]. The quadrature method is one of the more popular techniques for estimating modal

parameters because it is easy to use, very fast and requires minimum computing resources. An example of quadrature picking method is illustrated in Figure 2-12. It is, however, sensitive to noise on the measurement and effects from adjacent modes [16].

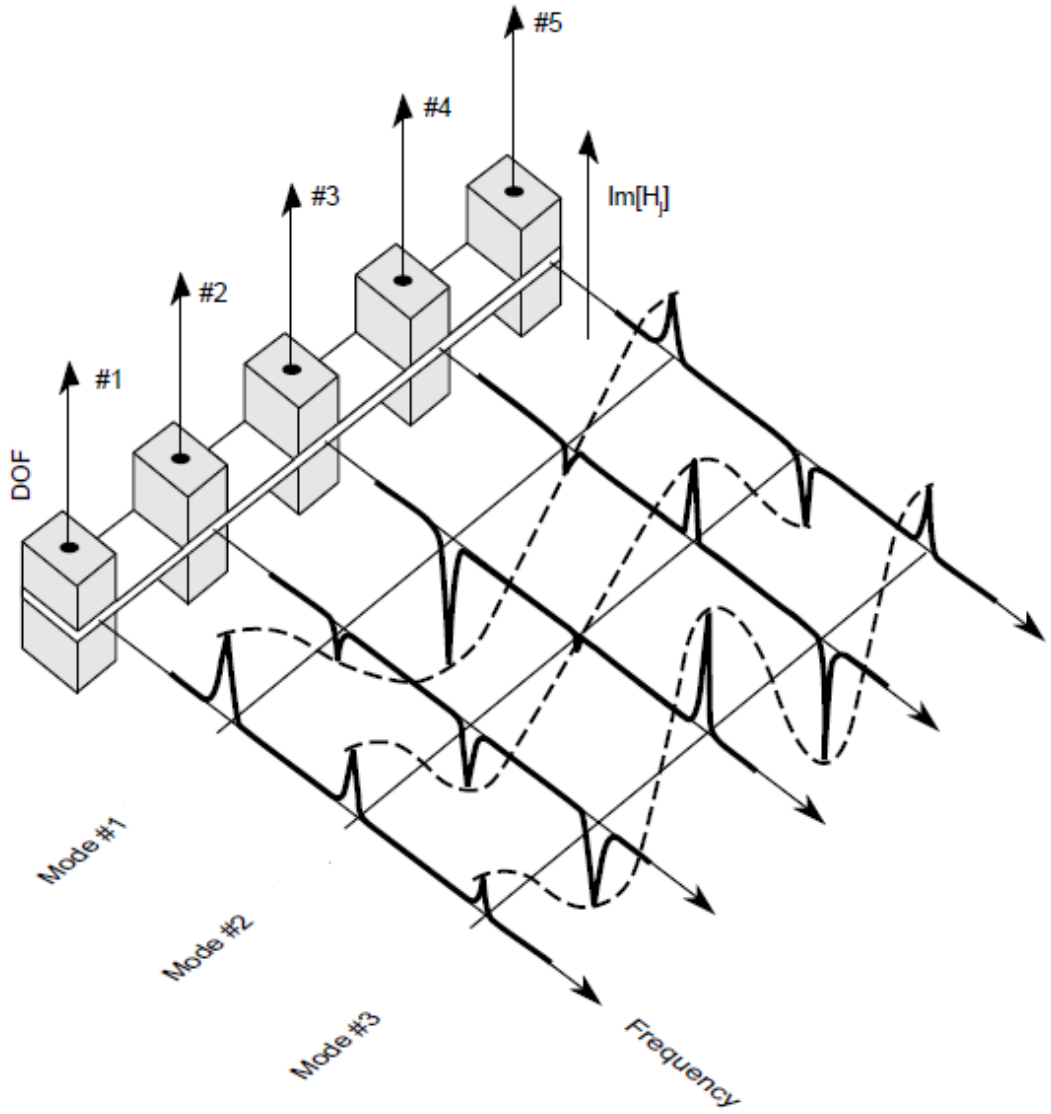

Figure 2-13: Modal coefficients estimation by the Quadrature Picking method

2.6 Fatigue

In general, fatigue can be defined as a phenomenon that takes place on components and structures subjected to time-varying external loadings and that manifests itself in the deterioration of the material's ability to carry the intended loading [18].

Fatigue occurs when a material is subjected to repeated loading and unloading. If the loads are above a certain threshold, microscopic cracks will begin to form at the stress concentrators such as the surface, persistent slip bands (PSBs), interfaces of constituents in the case of composites, and grain interfaces in the case of metals [19].

It has been estimated that fatigue contributes to approximately 90% of all mechanical service failures. Fatigue is a problem that can affect any part or component that moves. Automobiles on roads, aircraft wings and fuselages, ships at sea, nuclear reactors, jet engines, and land-based turbines are all subject to fatigue failures [20].

2.6.1 Fatigue Life

The American Society for Testing and Materials (ASTM) defines fatigue life, N_f, as the number of stress cycles of a specified character that a specimen sustains before failure of a specified nature occurs [21].

To determine the strength of materials under the action of fatigue loads, specimens are subjected to repeated or varying forces of specified magnitudes while the cycles are counted until destruction. Several tests are necessary because of the statistical nature of fatigue, to increase the accuracy. The results are plotted in the form of a S-N diagram (or Wohler diagram), that has the fatigue strength as its ordinate and the number of cycles to rupture as abscissa, this last disposed in a logarithmic scale. A typical example of S-N curve is illustrated in Figure 2-14 (right) [22].

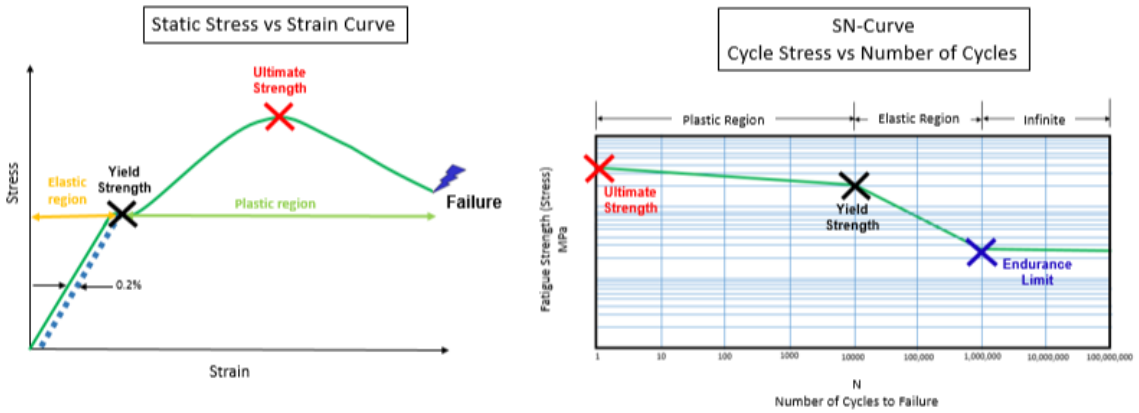

Figure 2-14: Typical S-N curve (right); Ultimate Strength and Yield strength can be determined from static stress-strain tests (left)

There are three key values that separate the plastic, elastic and infinite life regions (Figure 2-14):

- Ultimate Strength: Stress level required to fail with one cycle;
- Yield Strength: Dividing line between elastic and plastic region;
- Endurance Limit: If all cycles are below this stress level amplitude, no failures occur.

A S-N curve can contain several different areas: a plastic region, an elastic region and an infinite life region (Figure 2-14):

Infinite life region: Some materials, like steel, exhibit an infinite life region. In this region, if the stress levels are below a certain level, an infinite number of cycles can be applied without causing a failure (of course, no test has been performed for an infinite number of cycles in real life, but a million+ cycles is typical) [23]. Many non-ferrous metals and alloys, such as aluminum, magnesium, and copper alloys, do not exhibit well-defined endurance limits. Comparison of steel and aluminum S-N curves is shown in Figure 2-15.

Elastic region: the relationship between stress and strain remains linear. When a cycle is applied and removed, the material returns to its original shape and/or length. This region is also referred to as the "High Cycle Fatigue" region, because a high number of stress cycles, at a low amplitude, can cause the part to fail.

Plastic region: the material experiences high stress levels, causing the shape and/or geometry to change due to the repeated application of stress cycles. This region is also referred to as the "Low Cycle Fatigue" region of the S-N curve, where a low number of stress cycles, with a high amplitude, result in failure.

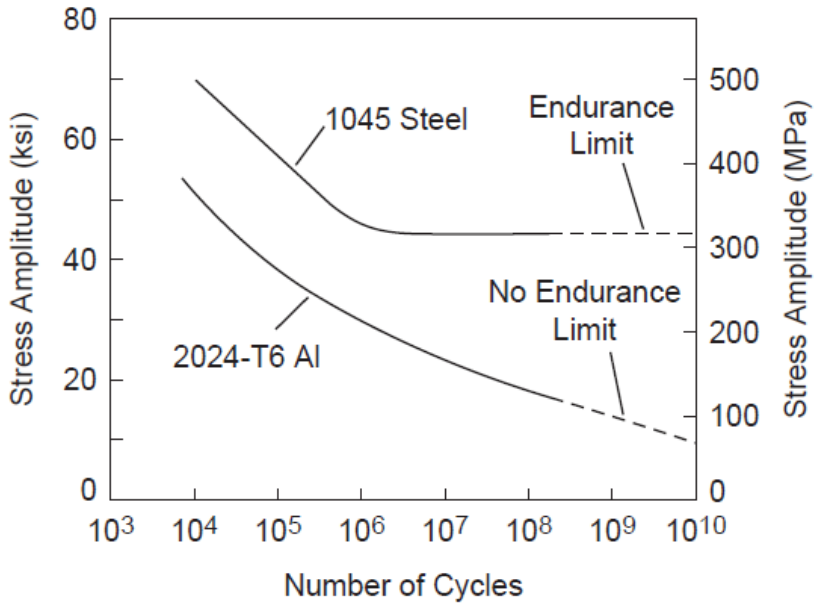

Figure 2-15: Typical S-N Diagrams of aluminum and steel alloys

2.6.2 Miner's Rule

Miner's Rule [24] is used to calculate damage caused by cyclic/time variant loading. It is a linear damage accumulation model that uses a load time history and S-N curve as inputs to calculate damage.

Miner's rule can be written as:

$$\boldsymbol{D} = \sum_{\boldsymbol{i}} \boldsymbol{d_i} = \sum_{\boldsymbol{i}} \frac{\boldsymbol{n_i}}{\boldsymbol{N_i}} \tag{31}$$

where $\boldsymbol{D}$ the cumulative damage, $\boldsymbol{d_i}$ is the fatigue damage in each cycle, $\boldsymbol{n_i}$ is the expected number of cycles at a stress level $\boldsymbol{\sigma_i}$, and $\boldsymbol{N_i}$ is the number of cycles to failure at that same stress level calculated from the S-N fatigue life curve.

When damage, $\boldsymbol{D}$, is equal to "1", failure occurs. The definition of failure for a physical part varies. It could mean that a crack has initiated on the surface of the part. It could also mean that a crack has gone completely thru the part, separating it.

2.6.3 Random Vibration Fatigue

In a random vibration analysis, it is assumed that the loading and response is statistical in nature and it can be represented by a zero-mean normal (Gaussian) distribution. It is sometimes convenient to view this distribution from the perspective of the likelihood that a certain level of load or response will fall within a certain standard deviation from the mean. Typically, we consider the $\boldsymbol{1\sigma}$, $\boldsymbol{2\sigma}$, and $\boldsymbol{3\sigma}$ (standard deviation or RMS) levels. As an example, given a random Gaussian loading, $\boldsymbol{x(t)}$, the probability that $\boldsymbol{x(t)}$ lies between $\pm\,\boldsymbol{1\sigma}$ is $\boldsymbol{68.3}$%, the probability that it lies between $\pm\,\boldsymbol{2\sigma}$ is $\boldsymbol{95.4}$%, and that for $\pm\,\boldsymbol{3\sigma}$ is $\boldsymbol{99.7}$%, as shown in Figure 2-16 [25].

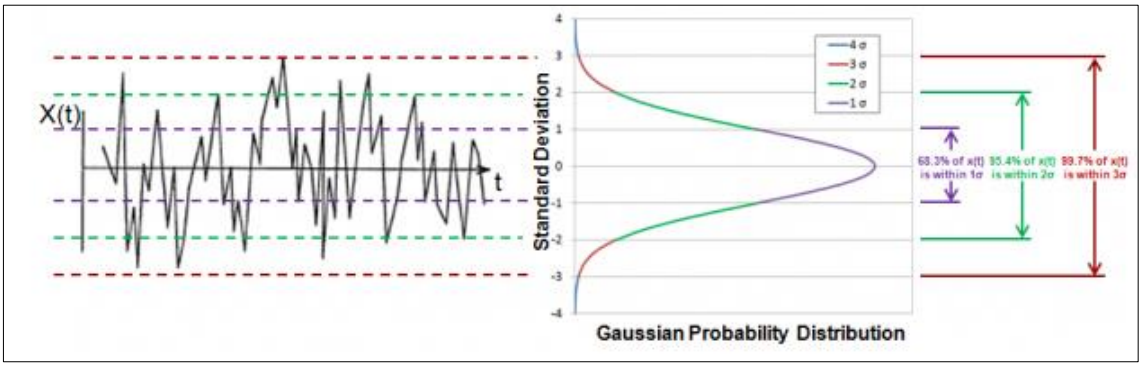

Figure 2-16: Gaussian distribution (right) of typical random signal (left)

Time-domain methods, using Rain-flow counting, can also be applied to random processes. However, analysis in the frequency domain is usually preferred due to the significant advantage from the perspective of numerical computation. There are many frequency-based methods that have been developed over the years which calculate damage based on a random vibration loading. These different methods employ various techniques that

calculate the fatigue life based on the $\mathbf{1\sigma}$ values that are typically calculated by the Finite Element Analysis. All the common methods used today are based on Miner's rule.

2.6.4 Steinberg 3-Band Method

The Steinberg 3-band method for damage calculation is frequently used due to its simplicity [26]. It uses a Miner's Rule approach to calculate cumulative fatigue damage by assuming that the stress amplitude response at a given location has a Gaussian distribution that's divided into the following three intervals:

- 68.3% of the time at $\boldsymbol{\sigma}$
- 27.1% of the time at $\mathbf{2\sigma}$
- 4.3% of the time at $\mathbf{3\sigma}$

In each of these intervals, the number of cycles to failure ($\boldsymbol{N_1}$, $\boldsymbol{N_2}$, and $\boldsymbol{N_3}$) can be determined from the material S-N curve, as shown in Figure 2-17. Then, if the total number of applied cycles "$\boldsymbol{n}$" is known, we can use the Steinberg 3-band method to determine the cumulative fatigue damage, D:

$$\boldsymbol{D = n\left(\frac{0.683}{N_1} + \frac{0.271}{N_2} + \frac{0.043}{N_3}\right)} \tag{32}$$

When all the life is used up, the value of $\boldsymbol{D}$ will be equal to 1.

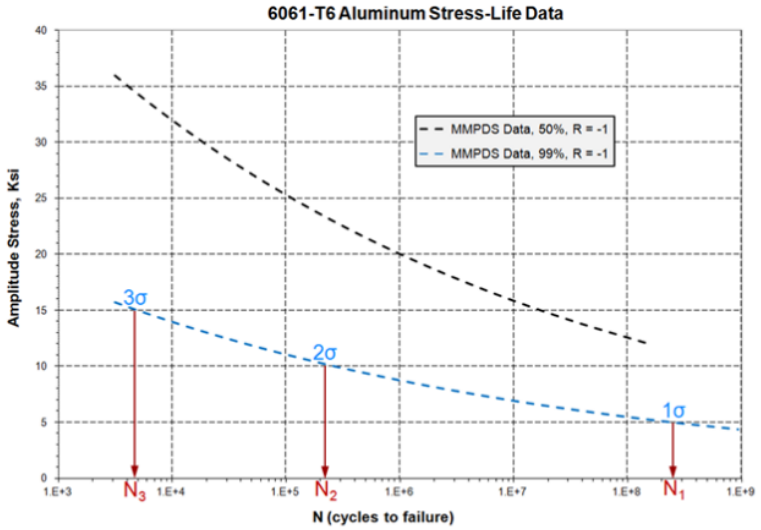

Figure 2-17: Number of cycles estimation method using Steinberg 3-Band Method

Steinberg's method is useful for illustrating the basic concept of fatigue analysis for random processes, but it has a couple of drawbacks which hinder its accuracy. Many other frequency domain methods are available, which produce much better correlation with rainflow-counting results for wide-band random response. Some of these include Wirsching-Light, the 0:75 method, Gao-Moan, Dirlik, Zhao-Baker, Tovo-Benasciutti and Petrucci-Zuccarello.

2.6.5 Miles Equation

Miles investigated fatigue failure of aircraft structural components caused by jet engine vibration and gust loading. Miles simplified his research by modelling a system using one degree of freedom. He also applied statistical recent results. While his goal was to analyze the stress of a component, the equation can be rearranged and used to determine, among others, displacement, force, and, in this case, acceleration.

Miles' Equation is derived using a Single Degree of Freedom (SDOF) system (lightly damped), consisting of a mass, spring and damper, excited by a constant-level white Noise random vibration input from 0 Hz to infinity. It states that the RMS of the output acceleration amplitude, $\boldsymbol{G_{RMS,out}}$, is:

$$\boldsymbol{G_{RMS,out}} = \sqrt{\frac{\boldsymbol{\pi}}{\boldsymbol{2}} \cdot \boldsymbol{f_n} \cdot \boldsymbol{PSD_{in}} \cdot \boldsymbol{Q}} \tag{33}$$

where $\boldsymbol{f_n}$ is the resonant frequency; $\boldsymbol{PSD_{in}}$ is the power spectral density function of the input acceleration; $\boldsymbol{Q}$ is the quality factor (section 2.2.4).

3 Experimental Tests

3.1 Test Bench

Experimental tests were performed using a test bench, shown in Figure 3-1, located in the DIMEAS Laboratory of Politecnico di Torino. The main hardware and software, and specimen characteristics used in these tests are described in this section.

Figure 3-1: Test bench

3.1.1 Hardware

The test bench is consisted of:

- Modal Shaker
- Amplifier
- Input and Output Instruments
- Accelerometers
- Clamping System

Modal Shaker

The device used to excite the specimens in the vibration tests was Dongling Modal Shaker model ESD-045. It's a compact system suited for micro-vibration tests since it has a permanent magnet inside, which allows it to be driven directly by the power amplifier analog signal and reduces the heat generation. Its technical specifications are displayed in Figure 3-2, [27].

SPECIFICATION	MODAL SHAKER
Sine force (peak)	450N
Usable Frequency Range	5 to 3000Hz
Max. Displacement	25 mm
Max. Velocity	1,6 m/s
Max Acceleration	1000 m/s²
Effective Mass of Moving Elements	450g
Weight	25kg
Dimension (L×W×H)	239 × 152 × 220 mm
Power Amplifier Model	PA – 1200
Cooling Type	Air-Cooled
Power Supply Requirement	AC 220V ± 10%, 50Hz, 1300VA
Working Environment Requirement	Temperature Range 0 – 40 °C Humidity range ≤ 80%

Figure 3-2: Modal shaker and its specifications

Amplifier

Dongling linear power amplifier PA-1200 is used to raise the power of the output analog signal to operate the Modal Shaker. Its technical specifications are displayed in Figure 3-3 , [28].

SPECIFICATION	AMPLIFIER
Rated Power (10 Ohms)	1200 W
Frequency Response	5 – 20kHz < ± 2dB
Signal-to-noise ratio	> 90 dB
Power supply	220 VAC 50Hz
Power consumption	2400 W
Weight	20kg
Dimensions (L×W×H)	480 × 740 ×132 mm

Figure 3-3: Power Amplifier PA-1200 and its specifications

Input and Output Instruments

Data transfer between the computer and the test bench equipment were done through the National Instruments compact modules: one NI 9234 for input data transfer, and one NI 9263 for output data transfer.

Both the NI 9234 and NI 9263 are connected to the computer by an USB cable through one compact DAQ NI 9171 each (shown in Figure 3-4), that intermediates this connection.

The NI 9234 is an analog input module used to acquire data from the transducers, i.e. accelerometers. While the NI 9263 is an analog output module, used for sending the desired voltage signal to the Modal Shaker, passing through the power amplifier first. Their main specifications are shown in Figure 3-5 [29], [30].

Figure 3-4: NI 9171

SPECIFICATION	NI 9234	NI 9263
SIGNAL RANGE	±5V input	±10V output
CHANNELS	4 differential	4
SAMPLE RATE	51.2 kS/s/ch	100 kS/s/ch
SIMULTANEOUS	Yes	Yes
RESOLUTION	24-Bit	16-Bit
EXCITATION	2 mA	1 mA per channel
ISOLATION	None	Yes

Figure 3-5: NI 9234 (left) and NI 9263 (right) and their specifications

Accelerometers

Accelerometers are the most important instruments in this research since they are used to record the acceleration response of the specimen at certain points. Two Triaxial PCB TLB356A12 accelerometers were used; one was placed on the clamping element to record the base acceleration and the other one was placed on the tip of the specimen to measure the tip acceleration. Both accelerometers were connected to the channels of the input module NI 9234. Their specifications are mentioned in Figure 3-6 [31].

SPECIFICATION	MODEL TLB356A12
SENSITIVITY IN Z DIRECTION (±10 %)	102,4 mV/g – Tip accelerometer 98,8 mV/g – Base accelerometer
MEASUREMENT RANGE	±491 m/s² pk
FREQUENCY RANGE (±5 %)	0.5 to 5000 Hz
RESONANT FREQUENCY	≥ 25 kHz
BROADBAND RESOLUTION (1 TO 10000 Hz)	0.002 m/s² (RMS)
NON-LINEARITY	≤1 %
OVERLOAD LIMIT (SHOCK)	±49050 m/s² pk
TEMPERATURE RANGE (OPERATING)	-54 to +77 °C
EXCITATION VOLTAGE	18 to 30 VDC
CONSTANT CURRENT EXCITATION	2 to 20 mA
DIMENSION (L×W×H)	11,4 × 11,4 × 11,4 mm
WEIGHT (WITHOUT CABLE)	5,4g

Figure 3-6: Accelerometers PCB TLB356A12 and their specifications

A new calibration for both accelerometers was done by previous student's work, (Camille, [32]) because the last calibration was done in 2009. The new accelerometers sensitivities are:

- **Base accelerometer: 82.99 mV/g**
- **Tip accelerometer: 85.35 mV/g**

Clamping Elements

A clamping structure, shown in Figure 3-7, is used to fix the to the Modal Shaker. It is composed of two metallic supports and a set of four screws, nuts and washers that keep the specimen fixed between the supports. The lower element has a groove on its inner face, where the specimen is placed, to guarantee a proper fixation. The upper support covers them and the screws compress these two parts with the specimen between them firmly.

The mass of the lower part is *200,4g* and the mass the upper part *205,6g*.

The sketch of both parts is shown in Appendix B

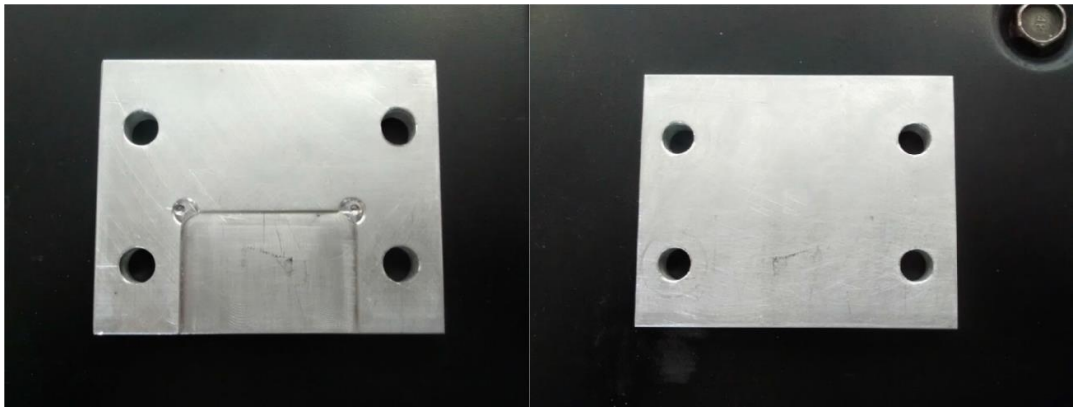

Figure 3-7: Lower (left) and upper (right) clamping elements

3.1.2 Software

The software used the most throughout the whole research was **LabVIEW** for its capabilities, simplicity and integration with physical platforms. It's based on a graphical programming syntax, with many built-in functions and procedures that permit signal and data generation, processing, output and acquisition, thus allowing system control in an effective and easier way. Besides that, LabVIEW has a great integration with the National Instruments hardware used in the test bench.

Another National Instruments' software used was **SignalExpress 2015**, that, like LabVIEW, allowed the tests to be done in an easier way because of its advantages in programming syntax too, but using a step-based syntax rather than graphical.

3.1.3 Specimen

The specimens used for the are made of steel alloy CP780, which is a common alloy in many industrial applications. Material specifications of the specimen will be discussed in section 3.2.

The specimen's geometry, as shown in Figure 3-8, was chosen based on previous researches and papers [15], [32], [33], [34], , [35], [36], [37], [38], [39], for two main reasons:

- its size is small enough; first to be analyzed with the available test bench equipment due to limitations of the Modal Shaker and the clamping structure, and then to have low stiffness as to avoid longer test times until its rupture.
- the notches are stress concentration points placed in specific zones in the specimen: the one closest to the clamped end (base), indicated as Notch 1, is highly deformed when excited in the second modal frequency, as it can be seen in Figure 3-9, as in that point the stresses are the highest. Therefore, the specimens are made to break exactly at Notch 1.

Each specimen was marked before the experimental test, as shown in Figure 3-8. A vertical line 32mm left to the base was made to guarantee the same clamping condition on each test, while on the tip end, the accelerometer's position was marked to place the accelerometer in a central position at the tip. Specimen sketch and dimensions are reported in Appendix C

The edges of Notch 1 were polished to avoid stress concentration due to superficial roughness from the fabrication process.

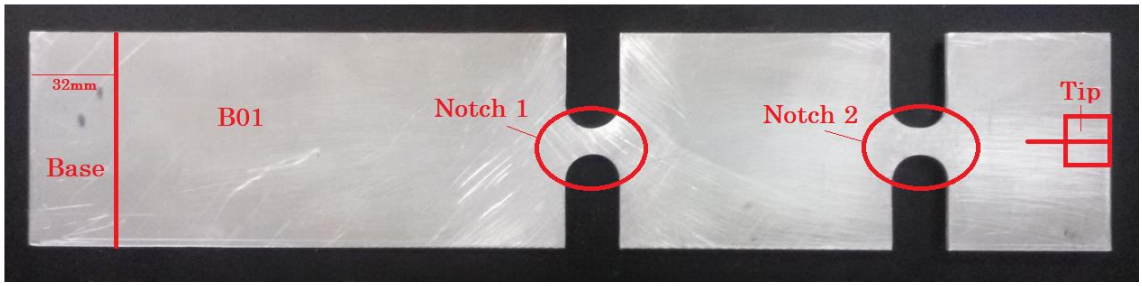

Figure 3-8: Specimen B01

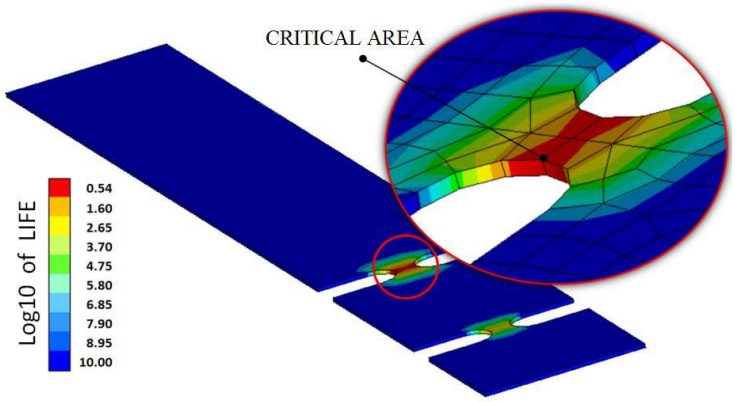

Figure 3-9: Stress concentration in Notch 1 when excited in second mode

3.2 Material

The material used in this study was the Complex Phase (CP) Steel CP780. The reason behind this choice is because steel alloys are vastly used in automotive industry for many components. It is a steel for complex shapes with energy absorbing capability and corrosion resistance. Galvanic corrosion protection of these zinc-based coated products makes them ideal for wet area components [40]. CP steels can be used in suspension system parts such as suspension arms [41].

3.2.1 Chemical Composition

The structure of these steels is a ferrite/bainite matrix containing martensite and small amounts of retained austenite and/or perlite. This creates a high yield strength tensile strength ratio. Chemical composition of the specimen material is reported in Table 3-1 [40].

Chemical Element	Composition %
%C max	0.18
%Si max	1
%Mn max	2.5
%P max	0.05
%S max	0.010
%Cr + %Mo max	1.00
%Nb + %Ti max	0.15
%Al max	0.015-1.00
%Cu max	0.2
%B max	0.005

Table 3-1: CP780 Chemical composition (ladle analysis in wt.%)

3.2.2 Mechanical Properties

Tensile Test

The mechanical properties of CP780 were extracted by a tensile test made using a specimen cut, as shown in Figure 3-10, according to the standards.

Figure 3-10: Tensile test specimen

The tensile test for CP780 was made by previous student's work (Camille, [32]), under the supervision of Prof. Sesana, with a servo-hydraulic testing

system INSTRON 8801. The specimen's deformation was measured with a strain gauge placed on central part of the deformed region.

As a result of this test, material's characteristic stress-strain curve is obtained as shown in Figure 3-11. From this graph, young's modulus, yield strength and the ultimate tensile strength, are extracted and they are reported in Table 3-2.

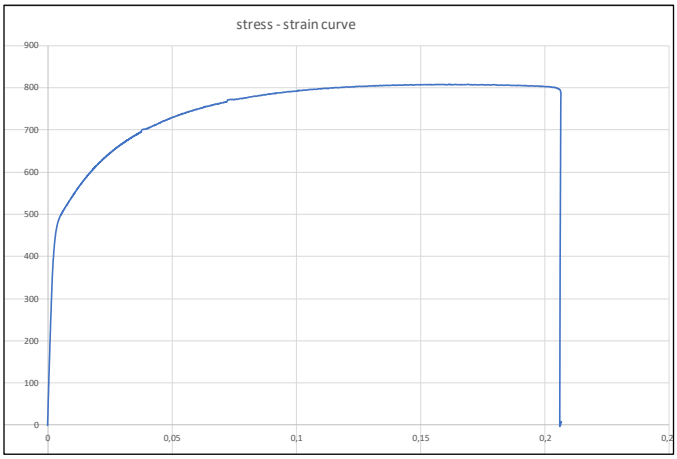

Figure 3-11: CP780 stress-strain curve

Mechanical Property	Value
Young's Modulus (E)	189.1-191.2 GPa
Yield strength ($R_{p0,2}$)	489-496 MPa
Ultimate tensile strength	809-810 MPa

Table 3-2: CP780 mechanical properties

Fatigue Strength

CP steels display high fatigue strength but they are more sensitive to severe strain peaks, i.e. abusive loads. Figure 3-12 gives examples of Wöhler curves for a variety of CP steels produced by ArcelorMittal. They are expressed as stress amplitude versus cycles to failure and are obtained with a stress ratio of R = 0.1 and repeated tensile loading [17].

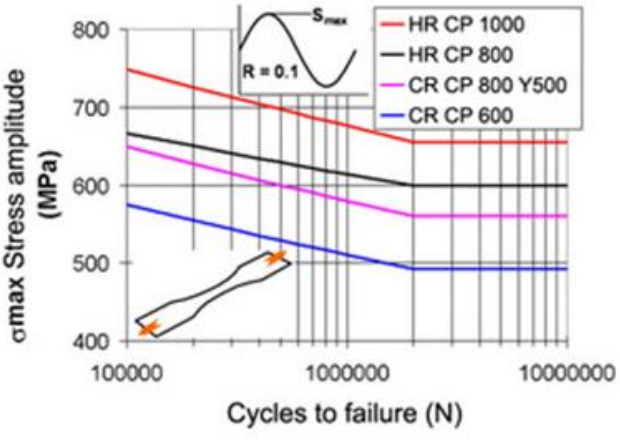

Figure 3-12: Wohler curves of different complex phase steels

3.3 Test Procedure

This test procedure was done by previous student's work (Costa Lima, [15]). In this section, only the main test procedure steps will be mentioned.

3.3.1 Test Setup

To perform the fatigue test, test bench elements must be placed as shown in Figure 3-13. Before starting, the specimen must be polished and its mass must be measured. Then, the specimen is clamped to the modal shaker by the clamping elements. With a special glue, two accelerometers are placed one on the base and the other on the specimen tip and they are connected to the computer through the dedicated National Instrument input modules (NI 9234) as described in section 3.1.1.

The Modal shaker is connected directly to the amplifier, which is connected also to the computer through the output modules (NI 9263).

After setting up the test bench, fatigue analysis test can be initiated. The specimen was subjected to several cycles of initial measurements, pre-test, followed by a "load block" for a certain amount of time controlled by the operator, and these cycles were repeated until the specimen's rupture. Both, the pre-test and the load block will be described in the following sections.

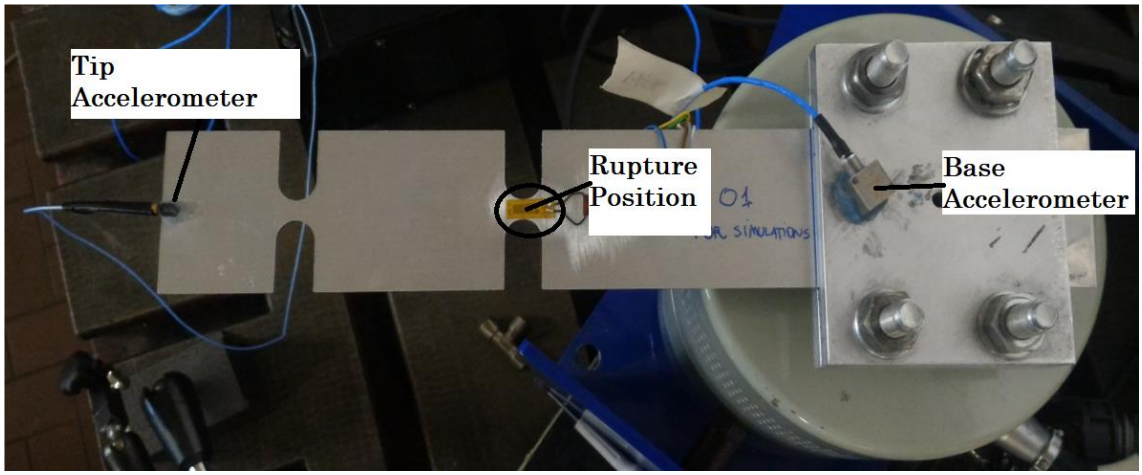

Figure 3-13: Test setup

3.3.2 Pre-Test

The aim of this test is to obtain the Reactance Frequency Response Function (FRF), according to the definitions described in section 2.3.4, which is used to extract the natural frequencies and the corresponding damping ratio of the tested specimen.

To do this, a SignalExpress program named "Shaker Test", Figure 3-14, is used. This program applies a wideband white Gaussian noise analog signal to the specimen through the modal shaker. Simultaneously, it measures the specimen's tip acceleration response by the tip accelerometer. As a result, the specimen's Inertance FRF is measured taking the excitation force that acts on the clamped region as input, and the specimen's tip acceleration as output.

The excitation force is calculated using Newton's 3rd law:

$$\boldsymbol{F(t) = m_{specimen} \cdot a_{base}(t)} \tag{34}$$

where $m_{specimen}$ is the specimen's mass, in kilograms, and $a_{base}(t)$ is the measured base acceleration.

As previously discussed, the output analog voltage signal sent to the modal shaker must pass first through the power amplifier. The amplification factor must be set according to predetermined value, as every specimen is going to be tested at different amplification factor.

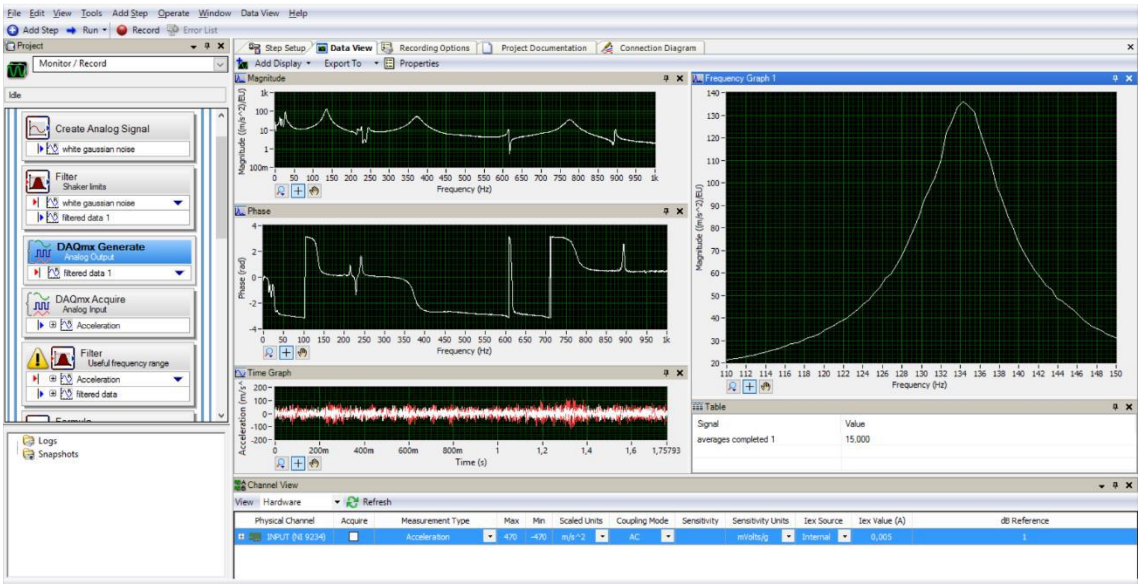

Figure 3-14: Frontal panel of the "Shaker Test" program

Other program's settings, as mentioned in [15], are reported in Table 3-3.

Setting	Value
Noise output signal amplitude	1V
Noise output signal filter	4th order lowpass filter
Noise cut-off frequency	3000 HZ
Accelerometers input signal filter	3rd order bandpass filter
Accelerometers signal cut-off frequencies	10 – 3000Hz
FRF: window	Hanning
FRF: number of averages	15

Table 3-3: "shaker test" program settings

Since the Reactance FRF is the desired quantity, it can be obtained from the Inertance (Accelerance) FRF using a LabVIEW program designed for this purpose, Figure 3-15 . As a result, both the reactance magnitude and phase spectra can be saved as text files.

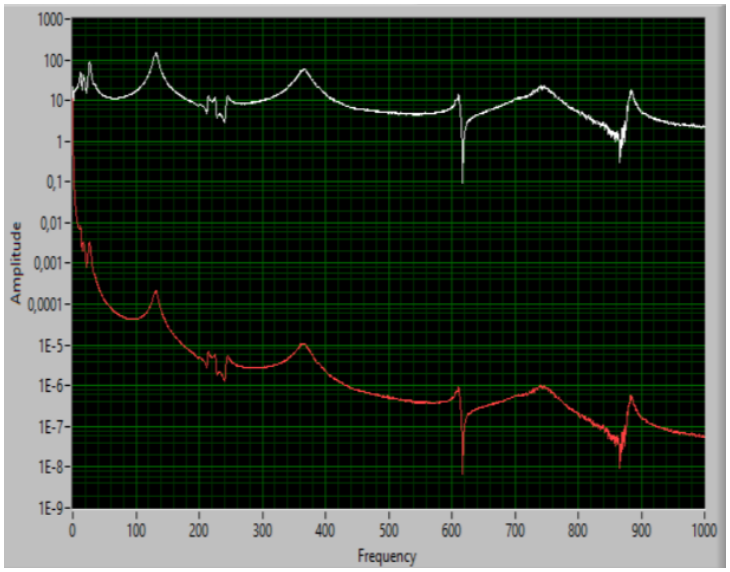

Figure 3-15: Inertance FRF (white) converted into Reactance FRF (red).

Now, having the reactance FRF, specimen's modal parameters, i.e. modal frequency and modal damping, are estimated by a LabVIEW program named "Modes Estimation", which uses a built-in block called MP_Peak_Picking.vi.

This Sub-VI uses the half-power bandwidth method to estimate the modal damping from the manually selected resonant frequency. The procedure is to select a frequency range of interest around a specific mode and it simulates the single degree of freedom system (SDOF) that best approximates that spectrum portion, based on the peak frequency chosen by the user inside that range.

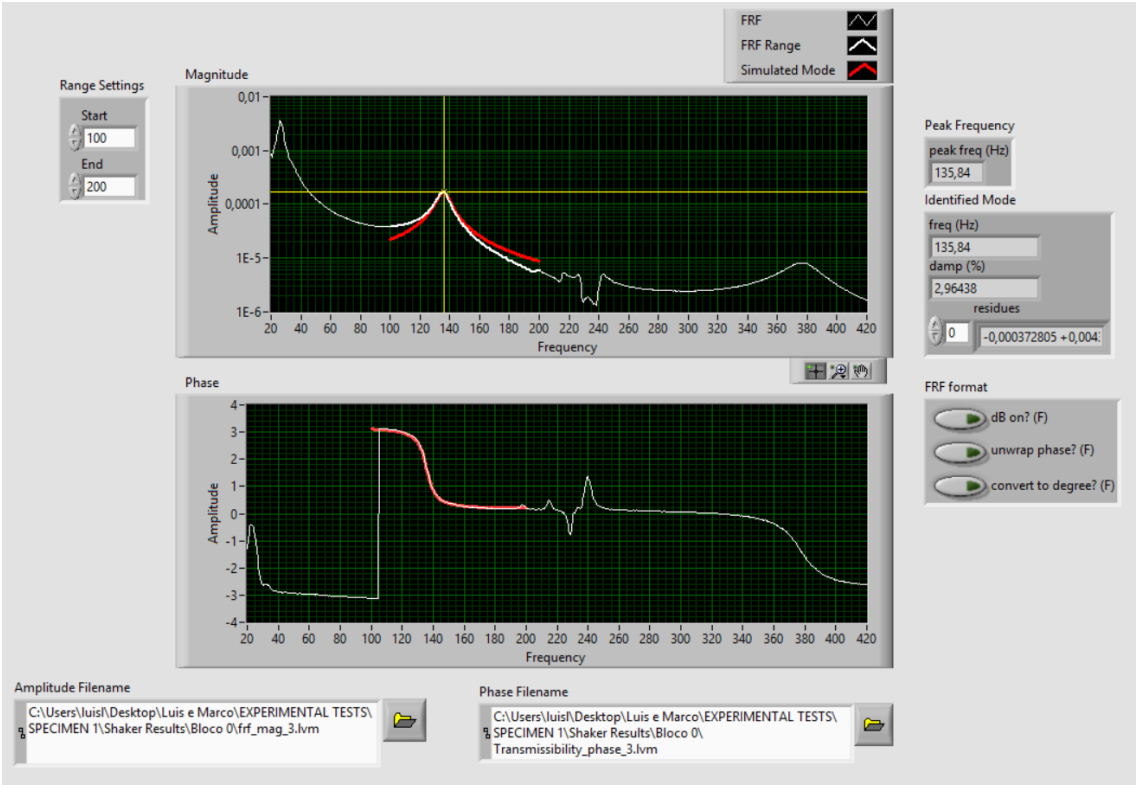

Figure 3-16: Front panel of the LabVIEW program "Modes estimation".

In this thesis, only the second mode is analyzed because the specimen is designed to break in Notch 1, as previously mentioned in section 3.1.3, which corresponds to the point that has the largest stresses when excited in the second mode, as shown in the upper right picture of Figure 3-17, [15].

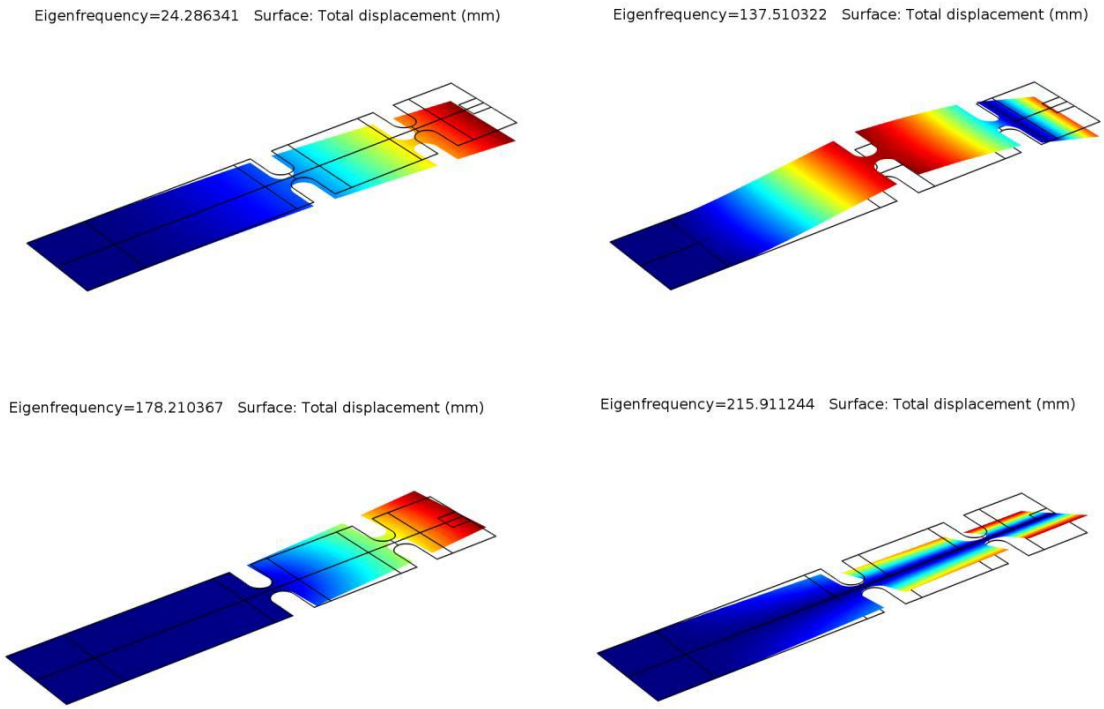

Figure 3-17: First four modes of the model

3.3.3 Load Blocks

Summarizing what is done till now; first the Inertance FRF (IFRF) was obtained using "Shaker Test" program, and the IFRF magnitude and phase are saved as external files. These files are the inputs of another LabVIEW program which calculate the Reactance FRF (RFRF). Then, using the LabVIEW program "Modes Estimation", the second mode frequency and the corresponding modal damping are obtained and recorded as Block 0. This procedure is called the PRE-TEST. It is important to note that in the pre-tests, both accelerometers must be placed as described in Figure 3-13.

After the pre-tests another test was performed, the Load blocks. Its purpose is to subject the specimen to a specific random acceleration load through the Modal Shaker for time desired by the operator.

It was made using LabVIEW programs called "Accelerometer Test", Figure 3-18. It generates a random Gaussian noise signal with a certain standard deviation (which is related to the load magnitude). This signal then passes through a bandpass filter to excite the specimen only within a specific frequency range, namely around the second resonant frequency. To make the tests feasible in terms of time, the frequency range must not be too wide nor too narrow as it would cause resonance and the specimen might break in a few minutes. A frequency range ±20 was considered in this thesis.

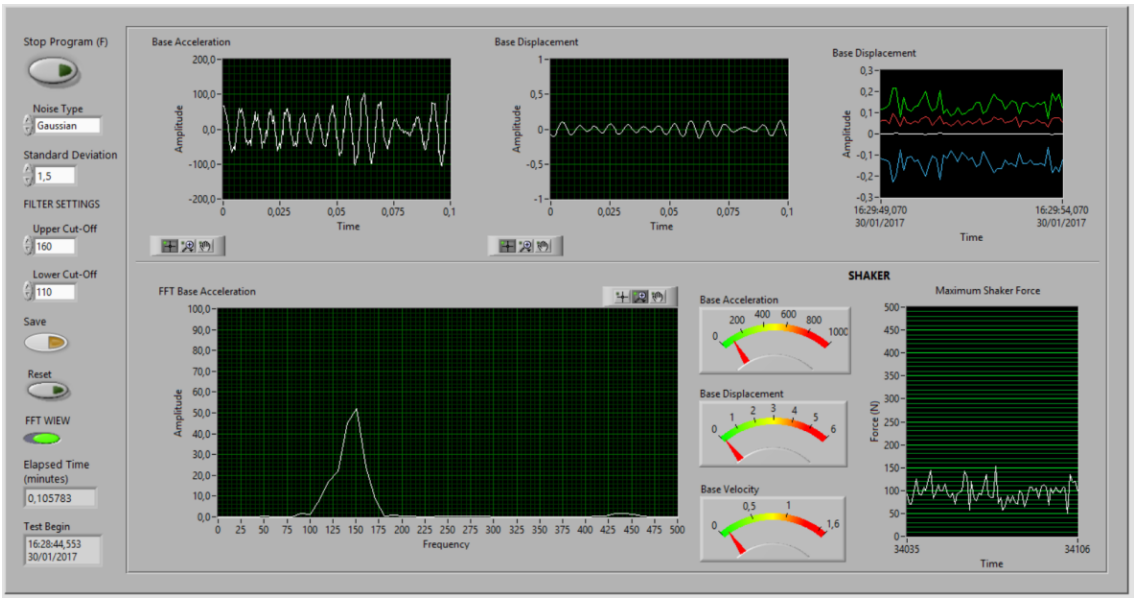

Figure 3-18: Frontal panel of the "Accelerometer Test" program

In the program's front panel, Figure 3-18, it can be set the type of the random acceleration signal (Gaussian noise was used), the value of the standard deviation (value of 2 is chosen by [15]), the bandpass filter's upper and lower cut-off frequencies, and the desired test duration.

During the load block test, the tip accelerometer was removed, keeping only the base accelerometer. However, it was kept only for few second at the starting of each load block test to record the specimen tip acceleration. The acceleration values from both accelerometers were saved in an external file as to be used later in data processing.

Load block test was repeated for fixed time duration (1 hour) until the specimen breaks, of course at notch 1. It is important to note that after each load block test, the pre-test was done again to obtain the new natural frequency and damping ratio. These new values were recorded as Block X, where X is the number of the previous load block test done. For example: Block 2 FRF measurements means that the second mode frequency and modal damping are obtained by the pre-test after completing the second load block test (as a total, the specimen is tested until now for two hours).

Finally, the tests sequence is represented on the flowchart in 0

3.4 Test Plan

Following the test procedure described in section 3; 30 CP780 steel specimens were available for testing. They were numbered B01, B02…B30.

The goal was to do the test at three different amplification factors. For each amplification factor, three different specimens must be tested. In total, I had to perform the test for nine different CP780 specimens. Each specimen was tested according to procedure described, until its rupture.

Load block tests were done according to the setting reported in Table 3-4, where f_n is the second mode natural frequency obtain from the pre-test.

Setting	Value
Applied signal	*White gaussian noise*
Standard deviation	2
Lower cut-off frequency	$f_n - 20\ Hz$
Upper cut-off frequency	$f_n + 20Hz$
Test duration	1 *hour*
Acceleration data recording duration[1]	60 *seconds*

Table 3-4: "Accelerometer test" program settings

3.4.1 Acceleration Profile

During each load block test, samples of the excitation acceleration were taken, by recording for 60 seconds the base acceleration measured with the base accelerometer. Figure 3-19 shows the probability density function (PDF) of specimen B05 base acceleration. It is well-approximated to a zero-mean Gaussian distribution (in orange), confirming the assumption of a Gaussian noise. A similar analysis can be done for the tip acceleration of B05 measured by means of the tip accelerometer, as shown in Figure 3-20.

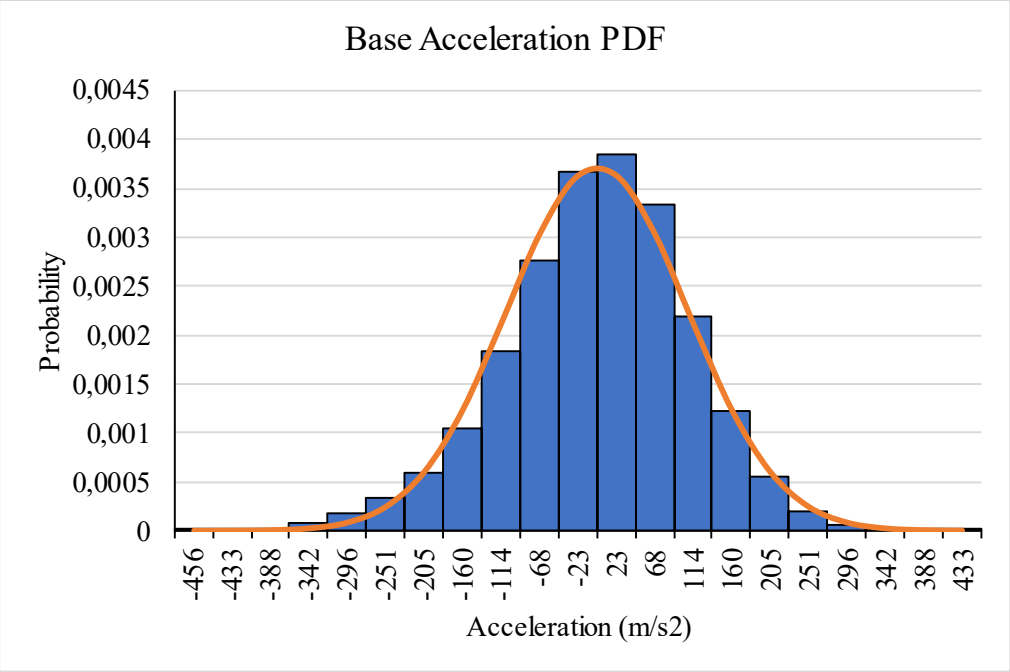

Figure 3-19: PDF of the base acceleration of specimen B05.

[1] The acceleration data recording duration is the time desired to record the acceleration values from the tip and base accelerometers. The recorded values are saved in an external file for further use.

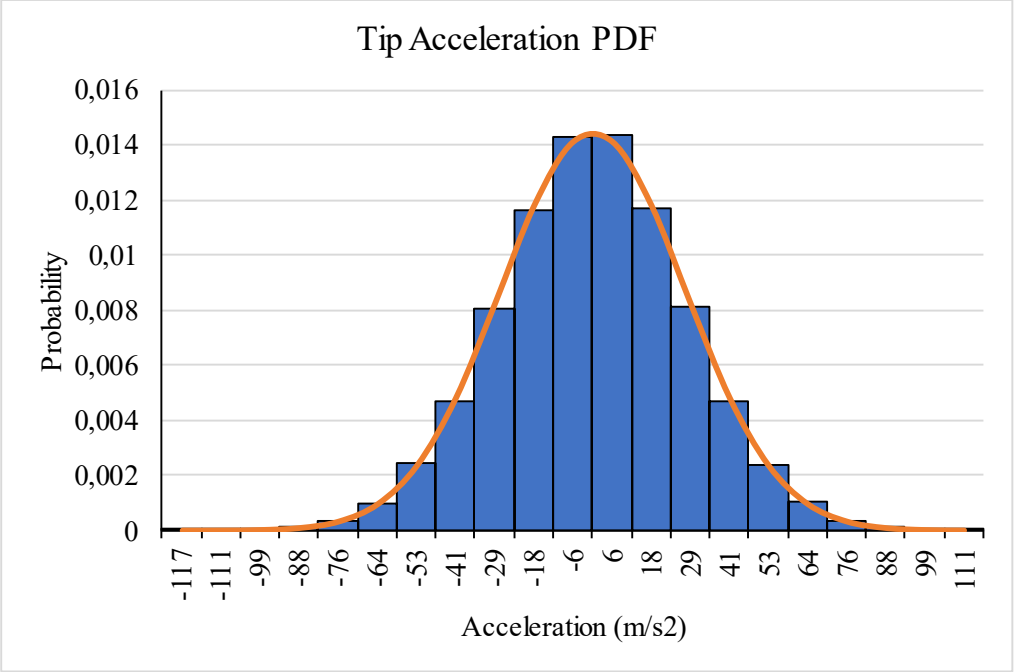

Figure 3-20: PDF of the tip acceleration of specimen B05

3.4.2 Amplification Factor

As already said, tests must be done for different amplification factor. Rotating the amplifier wheel, amplifier can be set for different values.

Amplifier PA-1200 described in section 3.1.1, has amplification range between 0 and 10. In this thesis, we want to consider only three amplification factors. In this subsection we will discuss how these three factors were determined.

Applying an amplification factor of value equal to 2, the specimen did not vibrate because the output signal was too week. Therefore, our starting point was 2.5.

Four preliminary amplification factors were chosen. For each factor, one specimen was tested according to Table 3-5.

Specimen	Amplification Factor
B02	3
B03	3.5
B04	4
B05	2.5

Table 3-5: Preliminary amplification factors chosen

The results of specimens B02, B03, and B04 tests are reported in Table 4 3. The results of specimen B05 test are reported in Table 3-7.

Specimen		B02			B03			B04		
Amplification		3			3.5			4		
Mode	Block	Time (min)	Freq. (Hz)	Damp. (%)	Time (min)	Freq. (Hz)	Damp. (%)	Time (min)	Freq. (Hz)	Damp. (%)
2	0	0	73.89	2.11	0	69.56	2.68	0	77.75	3.14
	1	60	73.21	2.49	60	68.87	2.15	38	Rupture	
	2	60	72.50	2.75	56	Rupture				
	3	60	80.48	2.09						
	4	47	Rupture							
Total time (min)		227			116			38		

Table 3-6: B02, B03, and B04 specimens' tests results

Specimen		B05		Amplification		2.5		Mode		2	
Block	Time (min)	Freq. (Hz)	Damp. (%)	Block	Time (min)	Freq. (Hz)	Damp. (%)	Block	Time (min)	Freq. (Hz)	Damp. (%)
0	0	85.94	1.71	14	60	83.21	1.83	28	60	83.21	1.87
1	60	83.89	1.50	15	60	82.53	1.69	29	60	83.21	1.87
2	60	85.26	2.15	16	60	83.21	2.22	30	60	83.21	1.69
3	60	85.26	1.75	17	60	83.21	1.88	31	60	83.21	1.69
4	60	84.58	1.79	18	60	83.21	1.77	32	60	83.89	1.65
5	60	84.58	1.98	19	60	83.21	2.15	33	60	83.89	1.65
6	60	83.89	1.58	20	60	83.21	2.10	34	60	83.21	1.65
7	60	83.89	2.39	21	60	83.21	1.98	35	60	83.21	1.65
8	60	83.89	1.89	22	60	83.21	2.00	36	60	83.21	1.65
9	60	83.89	1.68	23	60	83.21	1.87	37	60	83.21	1.65
10	60	83.89	1.50	24	60	83.21	2.05	38	60	83.21	1.65
11	60	83.89	1.22	25	60	83.21	2.22	39	60	83.21	1.65
12	60	83.21	1.86	26	60	83.21	2.18	40	60	83.21	2.16
13	60	83.21	1.92	27	60	83.21	1.66	Total		2400 min	

Table 3-7: B05 specimen's tests results with amplification factor 2.5

As it can be observed from Table 3-6, setting the amplifier for value equal to 4, the specimen broke in less than one hour, more precisely in 38 minutes. This result may not be accepted because we need to perform the fatigue test for longer time to analyze the results later.

For amplification factor equals to 2.5, 40 load block tests were done, i.e. the specimen was tested for 40 hours. Unfortunately, the specimen did not break.

Finally, the three amplification factors selected are 2.75, 3, and 3.25.

3.5 Test Results

The experimental tests were performed for nine specimens, each three specimens with one amplification factor, as described in Table 3-8.

Specimen	Amplification Factor
B10, B11, B18	2.75
B12, B13, B14	3
B15, B16, B17	3.25

Table 3-8: Experimental test specimens

After each load block test (of one hour), the modal parameters, i.e. the second modal frequency and modal damping are obtained by performing the pre-test, and the results are recorded as shown in Table 3-9, Table 3-10, and Table 3-11. It is important to note that the modal parameters in Block 0 are the initial values.

Amplification factor = 2.75

Specimen		B10			B11			B18		
Mass (g)		115.9			117.3			116.7		
Mode	Block	Time (min)	Freq. (Hz)	Damp. (%)	Time (min)	Freq. (Hz)	Damp. (%)	Time (min)	Freq. (Hz)	Damp. (%)
2	0	0	88.67	2.48	0	90.72	2.25	0	85.94	2.44
	1	60	85.26	2.81	60	90.72	2.25	60	83.89	2.52
	2	60	85.26	1.95	60	90.72	2.25	60	83.89	2.52
	3	60	85.26	1.95	60	90.72	2.25	60	83.89	2.25
	4	60	85.26	1.95	8	Rupture		60	83.89	2.25
	5	5	Rupture					60	83.89	2.89
	6							60	83.89	2.89
	7							40	Rupture	
Total time (min)		245			188			400		

Table 3-9: B10, B11, and B18 specimen tests with AF 2.75

Amplification factor = 3

Specimen		B12			B13			B14		
Mass (g)		114.6			116.8			116.4		
Mode	Block	Time (min)	Freq. (Hz)	Damp. (%)	Time (min)	Freq. (Hz)	Damp. (%)	Time (min)	Freq. (Hz)	Damp. (%)
2	0	0	85.26	2.40	0	84.58	2.74	0	85.94	1.96
	1	60	83.21	2.50	60	83.21	2.33	60	85.94	2.28
	2	60	83.21	1.96	60	82.53	2.21	60	85.94	2.62
	3	5	Rupture		19	Rupture		60	85.94	2.23
	4							48	Rupture	
Total time (min)		125			139			228		

Table 3-10: B12, B13, and B14 specimen tests with AF 3

Amplification factor = 3.25

Specimen		B15			B16			B17		
Mass (g)		116.9			116.9			116.8		
Mode	Block	Time (min)	Freq. (Hz)	Damp. (%)	Time (min)	Freq. (Hz)	Damp. (%)	Time (min)	Freq. (Hz)	Damp. (%)
2	0	0	86.62	2.64	0	84.58	2.62	0	87.31	2.35
	1	60	85.26	2.31	60	84.58	2.53	60	81.85	2.06
	2	21	Rupture		14	Rupture		1	Rupture	
Total time (min)		81			74			61		

Table 3-11: B15, B16, and B17 specimen tests with AF 3.25

A graphical representation of test duration of all the tested specimens is shown in Figure 3-21. In can be seen that increasing the amplification factor, the time required for specimen rupture decreases.

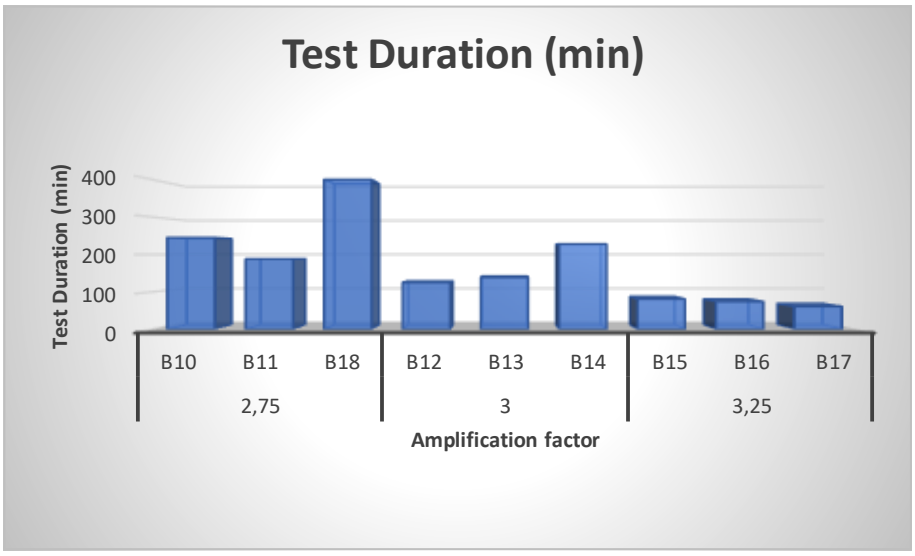

Figure 3-21: Test duration of tested specimens

4 Fatigue Analysis and Discussion

4.1 Data Processing

Starting from the acceleration time-histories obtained from both accelerometers, the tip accelerometer and the base accelerometer, and applying the fatigue models, described in section 2.6, the fatigue life of each specimen can be calculated by the procedure described below.

This procedure must be done for each load block in each specimen, and it consists of three main stages:

1. PSD analysis;
2. Stress calculation;
3. Fatigue analysis or fatigue life calculation.

These three stages are described in detail in the following subsections.

4.1.1 PSD Analysis

Random vibration environments, normally deal in terms of the power spectral density PSD, which is measured in gravity units [G] so that it is dimensionless. That is, the acceleration is divided by the acceleration of gravity [26]:

$$\boldsymbol{G = \frac{a}{g} = \frac{\text{acceleration}}{\text{gravity}}} \quad \text{(dimensionless)} \tag{35}$$

Random vibration PSD curves can come in a wide variety of shapes, depending on the type of condition the curve is trying to simulate. The square root of the area under the input/output PSD curve represents the input/output root mean square (RMS) acceleration level in gravity units [G].

In order to predict the probable acceleration levels, it is necessary to understand the probability distribution functions. The distribution most often encountered, and the one that lends itself most readily to analysis, is the Gaussian distribution. In our case, the input and output acceleration have zero-mean Gaussian distribution as it is shown in Figure 3-19 and Figure 3-20.

As it has been described in section 2.6.3, in Gaussian PDF, the probability that the instantaneous acceleration lies between $\pm \boldsymbol{1\sigma}$, which is the RMS value, is $\boldsymbol{68.3}$% of the time, the probability that it lies between $\pm \boldsymbol{2\sigma}$ is $\boldsymbol{95.4}$%, and that for $\pm \boldsymbol{3\sigma}$ is $\boldsymbol{99.73}$%.

The acceleration time-histories extracted from the experiments, were expressed in [m²/s]. Therefore, they should be converted to gravity units applying equation (35). The acceleration RMS value (standard deviation) in gravity units will now be expressed as G_{RMS}. What we are interested in, is the output (response) RMS acceleration $G_{RMS,output}$.

$G_{RMS,output}$ can be obtained experimentally from the acceleration time-history collected by the tip accelerometer, using Excel (built-in function STDEV.S).

Another method to calculate $G_{RMS,output}$ theoretically was used in previous students' works [35] [37] [36]. This time the response acceleration time-histories were missing. The method is based on Mile's Equation (section 2.6.5):

$$G_{RMS,output} = \sqrt{\frac{\pi}{2} \cdot f_n \cdot PSD_{in} \cdot Q} \tag{36}$$

From the input acceleration time-history, $G_{RMS,input}$ can be obtained. Then, the input power spectral density PSD_{in} can be calculated by:

$$PSD_{in} = \frac{G_{RMS,input}^2}{\Delta f} \tag{37}$$

where Δf is the Gaussian random vibration frequency band, in which specimens were excited (in our case $\Delta f = f_n \pm 20$, where f_n is the second mode natural frequency).

Q, presented in equation (36), is the transmissibility (or quality factor, section 2.2.4) at the natural frequency, and it can be obtained from equation the following equation:

$$Q = \frac{1}{2\zeta} \tag{38}$$

where ζ is the damping ratio. It is important to note that f_n and ζ were obtained from the experimental tests done.

In this thesis, both the experimental and the theoretical methods were used and a comparison between the results is reported in Table 4-1. It in can be seen that the ratio between the results, in each block, is approximately constant with an average value of 2.34.

Fatigue life calculations was done using both values.

AF	Specimen	Block	G RMS Response Exp.	Theor.	Ratio Theor/Exp
2.75	B10	1	12.16	26.18	2.15
		2	11.88	24.61	2.07
		3	12.58	25.67	2.04
		4	12.58	25.67	2.04
		5	12.58	25.67	2.04
	B11	1	12.52	27.85	2.22
		2	12.52	27.85	2.22
		3	12.52	27.85	2.22
		4	12.52	27.85	2.22
	B18	1	10.47	23.27	2.22
		2	10.47	23.27	2.22
		3	10.60	25.28	2.39
		4	10.60	25.28	2.39
		5	10.69	23.04	2.16
		6	10.69	23.04	2.16
		7	10.94	23.25	2.13
3	B12	1	15.50	35.03	2.26
		2	14.14	33.16	2.35
		3	14.15	34.09	2.41
	B13	1	14.96	34.04	2.28
		2	14.57	37.31	2.56
		3	14.61	37.70	2.58
	B14	1	11.91	31.23	2.62
		2	11.67	34.75	2.98
		3	11.64	28.30	2.43
		4	11.31	31.84	2.81
3.25	B15	1	16.43	37.87	2.30
		2	14.93	38.86	2.60
	B16	1	17.31	36.21	2.09
		2	16.95	36.23	2.14
	B17	1	16.88	37.90	2.25
		2	11.12	35.76	3.21
	Average				**2.34**

Table 4-1: G RMS response obtained experimentally and theoretically

4.1.2 RMS Stress Calculation

As said before, the most stressed point on the specimen is Notch 1. Therefore, in order to calculate the RMS bending stress, a lumped model for part A of the specimen, shown in Figure 4-1, is assumed. Part A is modelled as a cantilever beam of length $\boldsymbol{L}$ with a rectangular cross-section and a concentrated mass, $\boldsymbol{m_{eq}}$, at its free end.

$\boldsymbol{L = 0.121\ m}$ is the length of part A (Figure 4-1), and $\boldsymbol{m_{eq} = 0.445 * m_{specimen}}$ is the mass of part A in [kg]. Then, the RMS bending stress can be calculated as follows:

$$\boldsymbol{S_{1\sigma} = \frac{M}{I} Y \quad [MPa]} \tag{39}$$

where $\boldsymbol{I}$ is the second moment of area in [m^4], $\boldsymbol{Y}$ is the vertical distance away from the neutral axis in [m], and $\boldsymbol{M}$ is the bending moment in [N.m].

$\boldsymbol{Y = {}^{h}/_{2} = 0.000625\ m}$ where $\boldsymbol{h = 1.25mm}$ is the specimen's thickness.

The second moment of area $\boldsymbol{I}$ can be evaluated by:

$$\boldsymbol{I = \frac{bh^3}{12} = 1.156 * 10^{-12}\ m^4} \tag{40}$$

where $\boldsymbol{b = 0.0071\ m}$ is the notch length as shown in Figure 4-1.

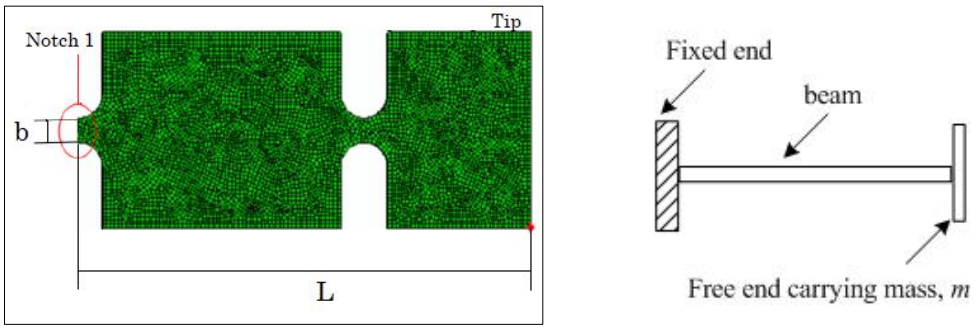

Figure 4-1: Part A of the specimen (left), and its lumped model (right)

The bending moment $\boldsymbol{M}$ can be obtained from the following equation:

$$\boldsymbol{M = K * m_{eq} * L * G_{RMS,output}} \tag{41}$$

$\boldsymbol{K}$ is the stress concentration coefficient. $\boldsymbol{K}$ can be used in the stress equation or in defining the slope b of the S-N fatigue curve for alternating stresses. The stress concentration should be used only once in either place. For this work, a stress concentration factor K=2 was used in the stress equation.

Once $\boldsymbol{S_{1\sigma}}$ is obtained, the stresses corresponding to the $\boldsymbol{2\sigma}$ and $\boldsymbol{3\sigma}$ acceleration levels are:

$$\begin{aligned} \boldsymbol{S_{2\sigma}} &= \boldsymbol{2S_{1\sigma}} \\ \boldsymbol{S_{3\sigma}} &= \boldsymbol{3S_{1\sigma}} \end{aligned} \tag{42}$$

4.1.3 Fatigue Analysis

For fatigue life calculation, root mean square (RMS) stress quantities, obtained from the previous step (subsection 4.1.2), are used in conjunction

with the standard fatigue analysis procedure. The following procedure, which consists of three steps, explains how to calculate the fatigue life using one of the most common approaches: The Steinberg 3-Band Technique (described in section 2.6.4) using Miner's Cumulative Damage Ratio (described in section 2.6.3) [26].

Step 1:

The first step is to determine the number of stress cycles needed to produce a fatigue failure. The approximate number of stress cycles, $\boldsymbol{N_1}$, $\boldsymbol{N_2}$, and $\boldsymbol{N_3}$ required to produce a fatigue failure in the specimen for the $\boldsymbol{1\sigma}$, $\boldsymbol{2\sigma}$ and $\boldsymbol{3\sigma}$ stresses respectively, can be obtained from the S-N diagram of the tested specimen. S-N diagram of specimen's material used can be estimated using Bastenaire Model, as shown in Figure 4-2 [37] [42]:

$$\boldsymbol{N = A\frac{exp\left[-\frac{\sigma-\sigma_d}{B}C\right]}{\sigma-\sigma_d}} \tag{43}$$

where $\boldsymbol{\sigma_d}$ is the endurance limit in [MPa]; For steel can be assumed as half the UTS, therefore from Table 3-2, $\boldsymbol{\sigma_d = 405\ MPa}$.

A, B, and C are parameters such that: A= 2.3E+07, B=165, and C=5.

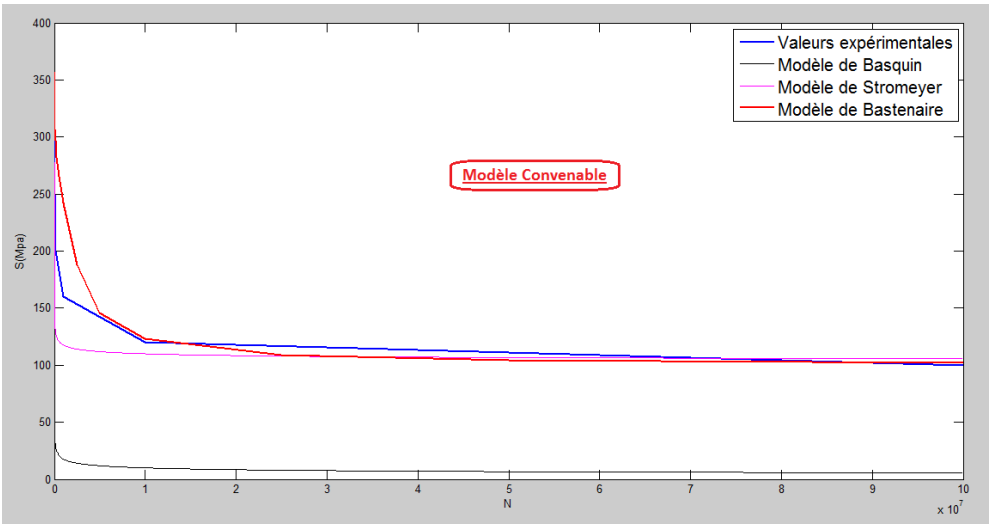

Figure 4-2: Modeling of the Wohler curve (blue) by the Bastenaire model (red).

Step 2:

From the Steinberg 3-Band method, the actual number of fatigue cycles $\boldsymbol{n_1}$, $\boldsymbol{n_2}$, and $\boldsymbol{n_3}$ accumulated during time, $\boldsymbol{t_{test}}$, of vibration testing can be obtained from the percent of time exposure for the $\boldsymbol{1\sigma}$, $\boldsymbol{2\sigma}$ and $\boldsymbol{3\sigma}$ stresses respectively, using the following equation:

$$\boldsymbol{n}\ [\text{cycles}] = \boldsymbol{f_n}[\text{Hz}] * \boldsymbol{t_{test}}[\text{sec}] * \frac{\%\boldsymbol{t_{exposure}}}{\boldsymbol{100}} \tag{44}$$

f_n is the specimen's natural frequency (in our case, the second mode). Considering 68.3% of the time at $\mathbf{1\sigma}$, 27.1% of the time at $\mathbf{2\sigma}$, and 4.3% of the time at $\mathbf{3\sigma}$, then we can obtain:

$$\begin{cases} n_{1\sigma} = f_n * t_{test} * 60 * 60 * 0.683 \\ n_{2\sigma} = f_n * t_{test} * 60 * 60 * 0.271 \\ n_{3\sigma} = f_n * t_{test} * 60 * 60 * 0.043 \end{cases} \quad (45)$$

Step 3:

Last step is to calculate the Miner's cumulative fatigue damage ratio. From the values obtained in step 1 and step 2, we can have:

$$d = \sum_{k=1}^{3} \frac{n_k}{N_k} = \frac{n_1}{N_1} + \frac{n_2}{N_2} + \frac{n_3}{N_3} \quad (46)$$

Note that, the damage ratio d, obtained above, is not the total damage ratio of the tested specimen. In fact, for each specimen, the damage ratio d must be calculated for every load block till rupture, and the total damage ratio is the summation of the obtained values.

Therefore, the total Miner's cumulative fatigue damage ratio is:

$$D_{total} = \sum_{i=1}^{m} d_i \quad (47)$$

where m is the number of the load blocks. As an example, the specimen B02, reported in Table 3-6, was tested for 4 load blocks, i.e. m is equal to 4.

4.2 Fatigue Analysis Results

Following the procedure described above, the results obtained for each specimen using both the experimental and the theoretical response GRMS, are reported in the following tables:

4.3 Discussion

5 Conclusion

Bibliography

[1] Data Physics Corp., "Vibration Testing and Shaker Testing," [Online]. Available: http://www.dataphysics.com/applications/vibration-testing-and-shaker-testing-shock-and-vibration.html. [Accessed 10 March 2018].

[2] S. M. Kumar, "Analyzing Random Vibration Fatigue," [Online]. Available: https://www.ansys.com/-/media/ansys/corporate/resourcelibrary/article/aa-v2-i3-random-vibration-fatigue.pdf. [Accessed 15 March 2018].

[3] D. G. Karczub and M. P. Norton, Fundamentals of Noise and Vibration Analysis for Engineers, Cambridge University Press, 2003, pp. 1-50.

[4] E. B. Magrab and B. Balachandran, Vibration, Cengage Learning, 2008.

[5] R. L. Eshleman, Basic machinery vibrations: An introduction to machine testing, analysis, and monitoring, 1999.

[6] S. S. Rao, Mechanical vibrations, Upper Saddle River, N.J: Prentice Hall, 2011, p. 556.

[7] L. Meirovitch, Fundamentals of vibrations, Boston: McGraw-Hill, 2001.

[8] S. S. Rao, Vibration of continuous systems, Hoboken, New Jersey: Wiley, 2007.

[9] R. Mancini and B. Carter, Op Amps for Everyone, Texas Instruments, p. 10–11.

[10] M. L. Stein, Interpolation of Spatial Data: Some Theory for Kriging, Springer, 1999, p. 40.

[11] F. Diebold, Elements of Forecasting, 4th ed., 2007.

[12] P. Avitabile, "Experimental Modal Analysis: A Simple Non-Mathematical Presentation," University of Massachusetts Lowell, Lowell, Massachusetts, 2001.

[13] R. Shamshiri and W. I. Wan Ismail, "Implementation of Galerkin's Method and Modal Analysis for Unforced Vibration Response of a Tractor Suspension Model," *Research Journal of Applied Sciences, Engineering and Technology. 7(1): 49-55.,* 2014.

[14] S. Gade, H. Herlufsen and H. Konstantin-Hansen, "How to Determine the Modal Parameters of Simple Structures," Brüel&Kjær, Denmark.

[15] L. H. Costa Lima, "Modal analysis on aluminium alloy subjected to random fatigue damage," Politecnico di torino, Torino, Italy, 2017.

[16] "The Fundamentals of Modal Testing," Agilent Technologies, 2000.

[17] M. Carfagni, E. Lenzi and M. Pierini, "The Loss Factor as a Measure of Mechanical Damping," in *SPIE – Proceedings of 16th International Modal Analysis Conference*, 1998.

[18] B. K. Sobczyk and J. F. Spencer, Random Fatigue: From Data to Theory, San Diego, CA: Academic Press, INC, 1992.

[19] W. H. Kim and C. Laird, "Crack nucleation and stage I propagation in high strain fatigue—II. mechanism," *Acta Metallurgica,* p. 789–799, 1978.

[20] F. C. Campbell, Elements of metallurgy and engineering alloys, ASM International, 2008.

[21] R. I. Stephens and H. O. Fuchs, Metal Fatigue in Engineering, John Wiley & Sons, 2001, p. 69.

[22] J. Hiatt, "What is a SN-Curve?," Siemens, [Online]. Available: https://community.plm.automation.siemens.com/t5/Testing-Knowledge-Base/What-is-a-SN-Curve/ta-p/355935. [Accessed 12 March 2018].

[23] C. Bathias, "There is no infinite fatigue life in metallic materials," *Fatigue & Fracture of Engineering Materials & Structures,* p. 559–565, 1999.

[24] M. A. Miner, "Cumulative Damage in Fatigue," *J. of Appl. Mech. Trans ASME,* pp. 159-164, 1945.

[25] E. Stamper, "How Do I Calculate Fatigue in a Random Vibration Environment? - Part 1," CAE Associates, [Online]. Available: https://caeai.com/blog/how-do-i-calculate-fatigue-random-vibration-environment-part-1#References. [Accessed 12 March 2018].

[26] D. S. Steinberg, Vibration Analysis for Electronic Equipment, 2nd ed., John Wiley and Sons, 1988.

[27] Dongling Technologies, *Vibration and Shock test solutions,* 2013.

[28] "PA and MP series amplifiers technical specifications," DONGLING TECHNOLOGIES, [Online]. Available: http://www.donglingtech.com/en/cp3-1-13_2.htm. [Accessed Aug 2017].

[29] National Instuments, *Datasheet: NI 9234,* October, 2015.

[30] National Instuments, *Datasheet: NI 9263,* March, 2016.

[31] P. Piezotronics, *Installation and Operating Manual - Triaxial ICP Accelerometer Model TLB356A12,* May, 2010.

[32] Camille Vaudelin, "Internship report," Politecnico di Torino, Torino, Italy, 2017.

[33] R. J. Siebra, "Random Fatigue Behaviour of Aluminum Alloy by means of Frequency Analysis," Politecnico di Torino, Torino, Italy, 2016.

[34] M. Quattrone, "Analysis of Aluminium Fatigue Life with Random Vibration Tests," Politecnico di Torino, Torino, Italy, 2015.

[35] A. Laghlabi, "Etude d'un essai de fatigue vibratoire en vue d'une correlation vibration/dommage," INSA, Blois, France, 2016.

[36] M. Delaplace, "Développement d'un banc d'essai de fatigue vibratoire en vue d'une corrélation vibration/fatigue," INSA, Blois, France, 2015.

[37] I. El Fakih, "Etude de la fatigue acceleree par severisation des essais vibratoires," INSA, Blois, France, 2016.

[38] G. d. M. Teixeira, "Random Vibration Fatigue Analysis of a Notched Aluminum Beam," *Int. J. Mech. Eng. Autom.,* vol. 2, no. 10, p. 425–441, Oct. 2015.

[39] M. Paiardi, "Modelli di danneggiamento a fatica random per leghe di alluminio," Politecnico di Torino, torino, Italy, 2016.

[40] Docol, "Docol 780CP Data Sheet," [Online]. Available: https://www.ssab.it/products/brands/docol/products/docol-780cp#!accordion=downloads. [Accessed 12 March 2018].

[41] ArcelorMittal, "Complex Phase Steels," [Online]. Available: www.totalmateria.com/page.aspx?ID=CheckArticle&LN=IT&site=kts&NM=372. [Accessed 12 March 2018].

[42] R. E. Little and J. C. Ekvall, Statistical Analysis of Fatigue Data, ASTM International, 1981.

[43] M. C. Jeruchim, P. Balaban and K. S. Shanmugan, Probability, random variables, and stochastic processes, Boston, MA: Springer, 2002.

[44] A. R. Crawford, The Simplified Handbook of Vibration Analysis, Computational Systems, Inc., 1992.

Appendix A Flowchart of Excitation Signals Types

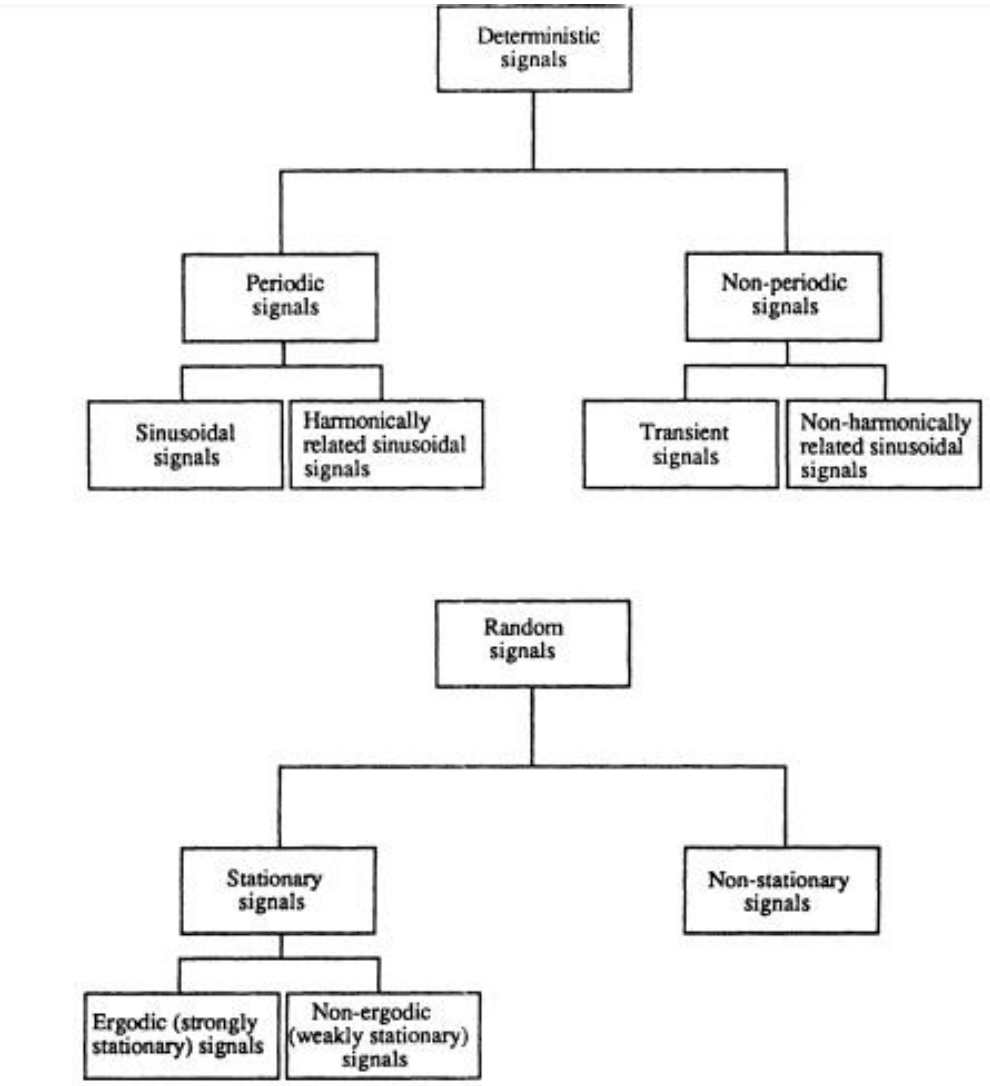

Appendix B Clamping Elements Sketch

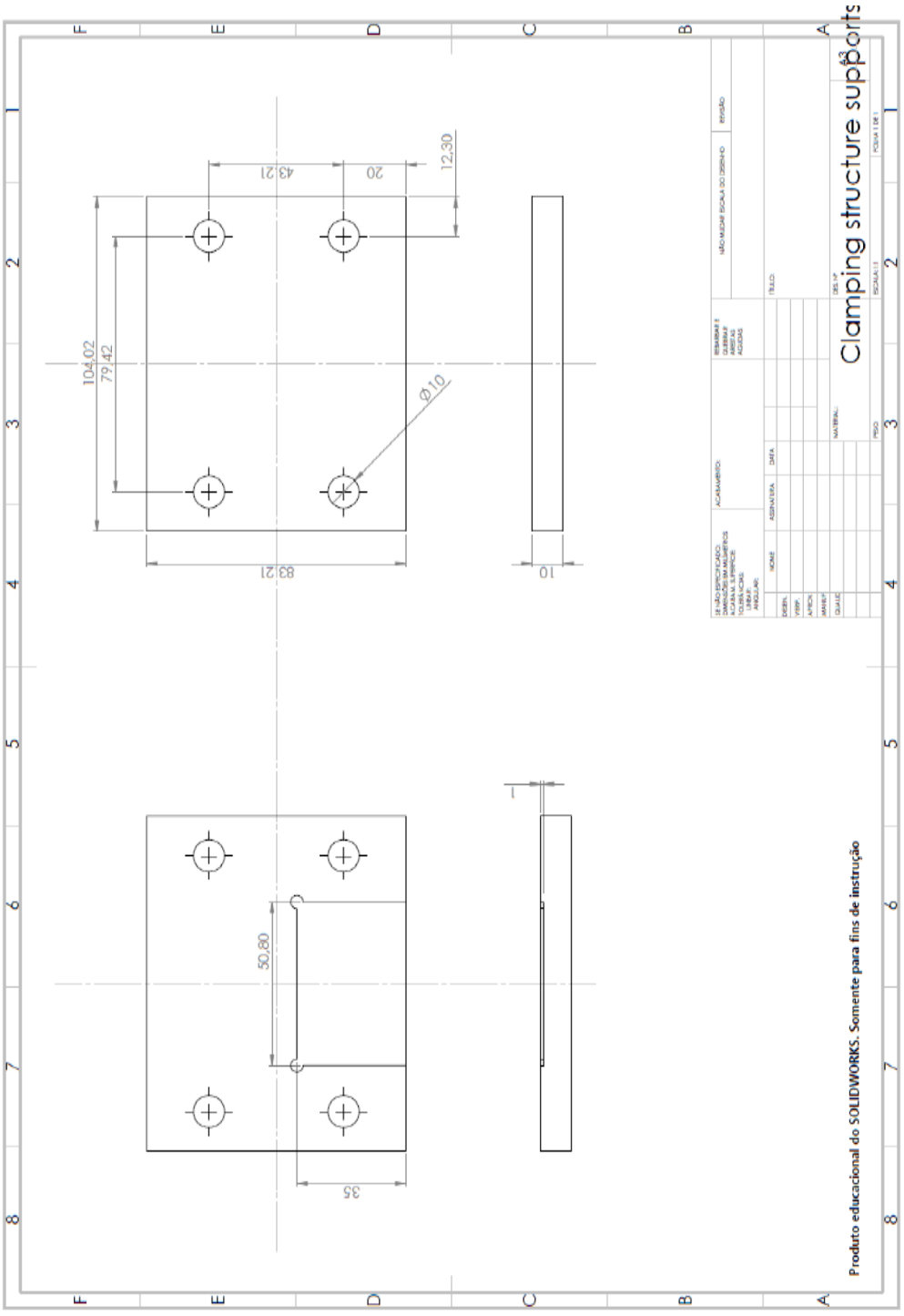

Appendix C Specimen Sketch

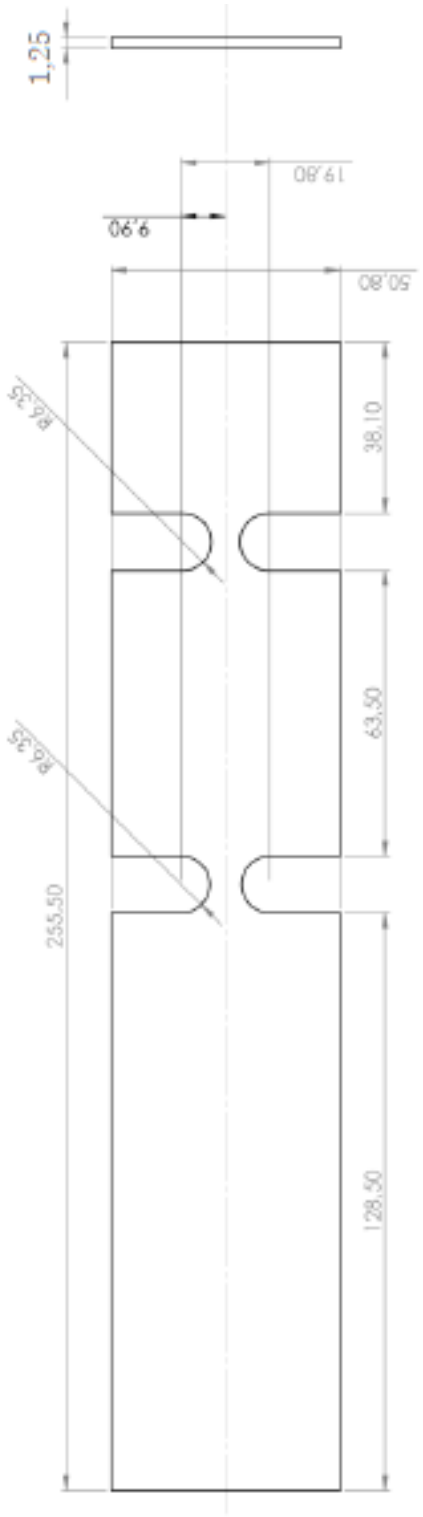

Appendix D Experimental Tests Flowchart